Nanostructured Europium and Palladium Oxide Substituted Lithium Manganese Oxide [$LiEu_{(x)}PdO_{(y)}MnO_3$] Perovskite Material for Li Ion Battery Cathode

UNIVERSITY *of the*
WESTERN CAPE

By

TUMISO EMINENCE MABOKELA (3972166)

A mini-thesis submitted in partial fulfilment of the requirements for the degree of

MAGISTER SCIENTIAE NANOSCIENCE

In the Faculty of Sciences, University of the Western Cape
Cape Town, South Africa

Supervisor: Prof Emmanuel I. Iwuoha

Co-Supervisors: Prof Kwena D. Modibane, Dr Chinwe O. Ikpo and Dr Assumpta C. Nwanya

June, 2021

DEDICATION

This work is dedicated to the memory of my loving grandparents:

John and Joyce Peter

DECLARATION BY CANDIDATE

I **TUMISO EMINENCE MABOKELA** declare that **NANOSTRUCTURED EUROPIUM AND PALLADIUM OXIDE SUBSTITUTED LITHIUM MANGANESE OXIDE MATERIAL FOR LI ION BATTERY CATHODE APPLICATION** is my own work and that all the sources that I have used or quoted have been indicated and acknowledged by means of complete references and that this work has not been submitted before for any other degree at any other institution.

Signature  ……

Date ……7 JUNE 2021……..

ACKNOWLEDGEMENTS

“Trust in the LORD with all your heart and lean not on your own understanding; in all your ways acknowledge Him, and He will make your paths straight.” - Proverbs 3:6

First and foremost, gratitude goes to God for the gift of knowledge, understanding and wisdom. I would also like to express my sincere gratitude to my supervisors Prof. Emmanuel Iwuoha, Prof. Kwena Modibane, Dr. Chinwe Ikpo and Dr. Nwanya for their support and encouragement during my studies. A word of thanks also goes to the Sensor Lab Research Group and the extraordinary team of researchers for their continuous help and support during my days in the lab. To my Sensor Lab mates, Emmanuel, Sinethemba, Shane, Kelechi, Onyi, Sodiq, Kaylin and Precious, thank you for making my days in the lab memorable. Thabang Somo, Peter Kganyago, Daniel Teffu and Siyabonga Mdluli, thank you guys for always availing yourselves to reviewing, correcting, and contributing to my research and thesis. To my friend Tshepo Sekgobela, thank you for helping me make memories at UWC and for standing by during those dark days. I would like to further thank my maternal family in the Western Cape for supporting me during my time at UWC, and my paternal family back in Limpopo for all your prayers, support and well wishes during my studies.

To the South African Department of Science and Innovation (DSI) and its National Nanoscience Postgraduate Teaching and Training Platform (NNPTTP) programme, a great thank you for the financial support throughout my studies.

ABSTRACT

The 4th Industrial revolution which is to be mainly powered by cleaner energy technologies has necessitated the scientific community to develop new high-tech energy storage materials. Furthermore, 4IR is associated with increased use of handheld and portable devices which require energy carriers such as supercapacitors and batteries with high power densities and high capacities. Although layered materials such as highly lithiated manganese oxides have paved the way in the development of new high-tech energy storage materials for Li-ion batteries, there is still huge room for improvements in such materials to achieve even greater electrochemical performance. It has been reported that highly lithiated manganese oxides can be modified using a variety of methods, such as surface coating, doping, and acid treatment to improve their stability and general electrochemical performance. Thus, this research focused on integrating these modification strategies to develop electrochemical superior highly lithiated manganese oxides to be applied as aqueous based Li-ion battery cathodes. In this work, europium doped highly lithiated manganese oxide Li_2MnO_3 were synthesized through sol-gel synthesis and electrochemically evaluated. The synthesized europium doped Li_2MnO_3 were then treated with mild HNO_3 as acid treatment, which has a synergistic effect on its electrochemical performance. Lastly, A jointly modified highly lithiated manganese oxide Li_2MnO_3 was fabricated by doping with europium and then decorating its surface with PdO via sonochemical methods to form a corrosion protective layer. The produced materials were characterized by Powder X-ray Diffraction (PXRD), Fourier Transform Infrared Spectroscopy (FTIR), Small Angle X-ray Scattering (SAXS), Inductively Coupled Plasma Optical Emission Spectroscopy (ICP-OES), High Resolution Scanning Electron Microscopy (HR-SEM), High Resolution Transmission Electron Microscopy (HR-TEM), and their electrochemical properties were evaluated using Cyclic Voltammetry (CV), Electrochemical Impedance Spectroscopy (EIS) and Galvanostatic Charge Discharge (GCD) in 1 M Li_2SO_4 electrolyte solution. The synthesized materials $Li_2Mn_{0.95}Eu_{0.05}O_3$, Acid treated $Li_2Mn_{0.95}Eu_{0.05}O_3$, and PdO@$Li_2Mn_{0.95}Eu_{0.05}O_3$ exhibited good electrochemical properties and yielded discharge capacities of 4.20, 17.8 and 6.4 $mAh.g^{-1}$ respectively.

RESEARCH OUTPUT

Publications

- **Mabokela, T.E.**, Nwanya, A.C., Ndipingwi, M.M., Kaba, S., Ekwere, P., Werry, S.T., Ikpo, C., Kwena, M. and Iwuoha, E., 2021. Recent Advances on High-Capacity Li Ion-Rich Layered Manganese Oxide Cathodes. *Journal of The Electrochemical Society*. (Published 16/07/2021) *See appendix 1*
- Somo, T.R., **Mabokela, T.E.**, Teffu, D.M., Sekgobela, T.K., Hato, M.J. and Modibane, K.D., 2021. Review on the effect of metal oxides as surface coatings on hydrogen storage properties of porous and non-porous materials. *Chemical Papers*, pp.1-15. (Published 05/01/2021) *See appendix 2*
- Somo, T.R., **Mabokela, T.E.**, Teffu, D.M., Sekgobela, T.K., Ramogayana, B., Hato, M.J. and Modibane, K.D., 2021. A Comparative Review of Metal Oxide Surface Coatings on Three Families of Cathode Materials for Lithium Ion Batteries. *Coatings*, *11*(7), p.744. (Published 22/07/2021) *See appendix 3*

TABLE OF CONTENTS

LIST OF FIGURES

LIST OF TABLES

LIST OF ABBREVIATIONS

AAS	: Atomic Absorption Spectroscopy
Ag/AgCl	: Silver-Silver Chloride Reference Electrode
BET	: Brauner-Emmett-Teller
CSIR	: Council for Scientific and Industrial Research
CV	: Cyclic Voltammetry
EDS/X	: Electron Dispersive X-ray Spectroscopy
EDTA	: Ethylenediaminetetraacetic acid
EIS	: Electrochemical Impedance Spectroscopy
EV	: Electric Vehicle
FTIR	: Fourier Transform Infrared Spectroscopy
GCD	: Galvanostatic Charge-Discharge
HF	: Hydrogen Fluoride
HR-SEM	: High Resolution Scanning Electron Microscopy
HR-TEM	: High Resolution Transmission Electron Microscopy
ICP-OES	:Inductively Coupled Plasma Optical Emission Spectroscopy
Li/Li^+	: Lithium metal Reference Electrode
Li-ion	: Lithium Ion
LRMO	: Lithium Rich Manganese Oxide
MS	: Mass Spectroscopy
NiCd	: Nickel Cadmium
Ni-MH	: Nickel-Metal Hydride
NMP	: 1-Methy-2-Pyrollidone
N_2O	: Nitrous Oxide
PdO	: Palladium Oxide
PVDP	: Polyvinylidene fluoride
PXRD	: Powder X-ray Diffraction
REE	: Rare Earth Elements
rGO	: Reduced Graphene Oxide
SAED	: Selected Area Electron Diffraction

SAXS	: Small Angle X-ray Spectroscopy
TGA	: Thermogravimetric Analysis
TM	: Transition Metal
USD	: United States Dollar
XPS	: X-Ray Photoelectron Spectroscopy
XRD	: X-ray Diffraction

LIST OF SYMBOLS

Å	: Angstrom
β	: Beta
R_{ct}	: Charge Transfer Resistance
Ω	: Ohm
γ	: Scan Rate
R_{SEI}	: Surface Film Resistance
θ	: Theta
λ	: Wavelength

CHAPTER 1

INTRODUCTION

1.1. Background of the Study

1.1.1. The global energy demands

The global energy demand is increasing at an alarming rate due to the rapid increase in the global population [1]. This rapid rise in the global population is associated with mounting industrialization and urbanization activities which have greatly increased the global energy demand [2],[3]. Currently, fossil fuel derived oil and gas play a major role in feeding this demand as estimates indicate that over 85% of the global energy demand is met by the burning of fossil fuels [4]. The transportation sector alone consumes over 30% of the global energy in the form of petroleum oil and gas [4], and it was reported that in 2017 approximately 64.5% of all the electricity generated was derived from oil, gas, and coal [6]. With the global population expected to rise even more to 8.5 billion in the year 2030, 9.7 billion in 2050 and 10.9 billion in 2100 [2], it is expected that more fuels will be needed to meet our rapidly increasing demand for energy.

1.1.2. The need for renewable energy

The use of fossil derived fuels to feed the ever-increasing demand for energy is becoming unsustainable and presents a myriad of environmental, economic, and health problems [7]. As depicted in figure 1.1, during the burning of fossil fuels, large amounts of greenhouse gases such as carbon dioxide (CO_2), methane (CH_4) and nitrous oxide (N_2O) are emitted into the atmosphere [7]. Naturally, these gases permit rays of light coming from the sun to reach the surface of the earth but trap the rays that are radiated back from earth surface [8]. As a result of the trapping of the reflected rays, the earth's average temperature increases, maintaining warm climatic conditions and this process is referred to as the greenhouse effect [8]. Scientists have reported that a more aggressive form of this phenomenon has been taking place around the world and is associated with increased greenhouse gas emissions from the burning of fossil fuels [9]. This human enhanced process has had some adverse effects on the

environment such as melting of sea and continent glaciers, rise in the sea level, severe drought and rising average global temperatures [9].

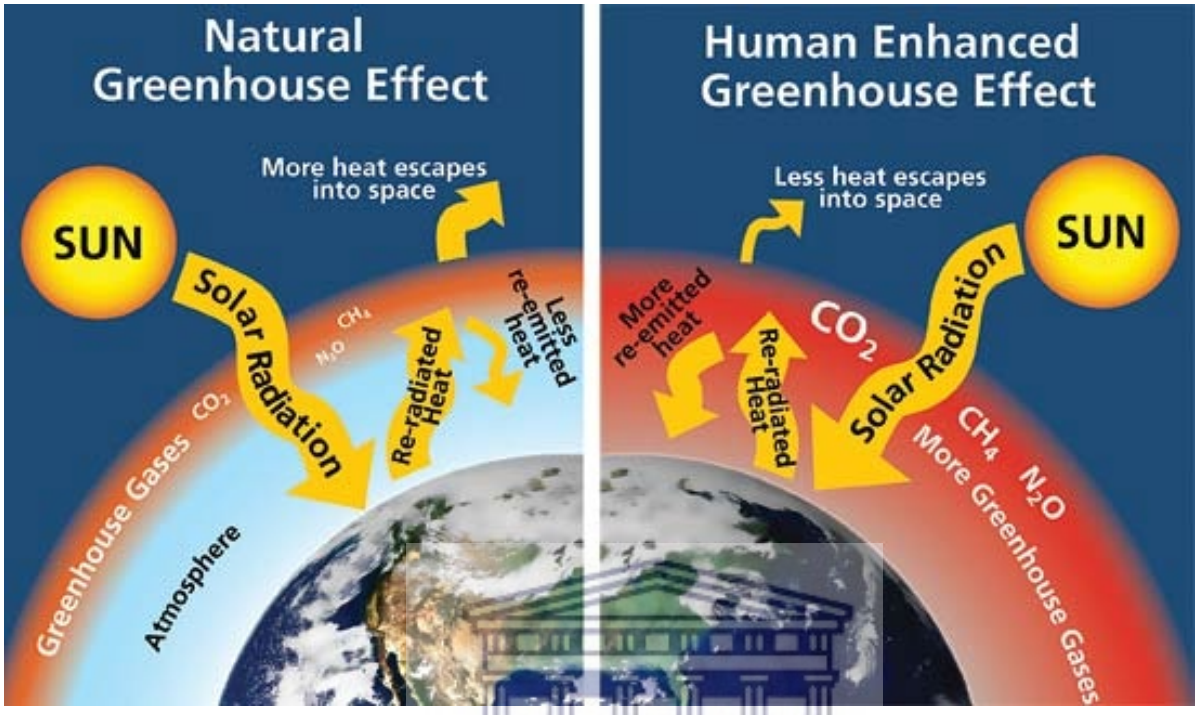

Figure 1.1: A comparison of the natural Greenhouse effect to human induced global warming [7].

Furthermore, the need for fossil fuels as primary sources of energy throughout the three industrial revolutions has triggered global socio-economic instabilities as rich countries scramble to increase their wealth. Consequently, the uneven distribution of global fossil fuel reserves raises concerns on 1) host country instabilities which can affect the oil price and 2) national energy security as a continuous and uninterrupted supply of energy is critical to the nation's economy [13]. Moreover, fossil fuels are non-renewable, and their complete depletion cannot be ruled out in the future [14]. Due to the above-mentioned factors, the scientific community has been tasked with the great responsibility of developing renewable and cleaner means of energy generation, to further mitigate climate change and environmental pollution associated with fossil fuel use.

1.1.3. The need for energy storage

To date, several renewable energy sources and technologies are being widely researched and developed as possible alternatives to the use of fossil derived fuels. For electricity generation, wind and solar energy which harness nature's clean energy have emerged as promising candidates due to their reduced carbon footprint in contrast to their non-renewable counterparts [15]. Despite being cleaner and cheaper per unit energy than fossil fuel derived oil, wind and solar energy generation also have limitations [3],[10]. The limitations lie in that the electricity generation is not constant but varies at different times and according to weather conditions. Thus electrochemical/mechanical energy storage systems are pivotal for wide range adoption of renewable energy sources and integration into the grid [11],[21]. On the other hand, electric and hybrid vehicles have shown great promise as possible alternatives to gasoline powered vehicles to curb and ultimately diminish the use of fossil fuels in the transportation sector [16]. Recently, the cost of owning an electric vehicle (EV) is on parity if not less than owning a gasoline powered vehicle when maintenance costs are factored in [17]. However, the feasibility of this technologies as replacements to conventional vehicles is challenged by the current cost of electric vehicle batteries and the battery life [18]. The realisation of the complete replacement of fossil fuels energy with cleaner energy sources is therefore dependent on the development of highly efficient energy storage technologies. There is ongoing research on implantation of different electrochemical energy systems in EVs and batteries as the favourite technology is maturing at an accelerated rate.

1.1.4. Lithium ion batteries for energy storage

Lithium ion batteries have attracted a great deal of attention in the research and development of large grid and electric vehicle energy storage systems [19],[20],[21],[24]. This is due to their higher specific energy, longer life span, power densities and their wide range of temperature versatility in applications in comparison to other commercial rechargeable batteries like lead acid, nickel cadmium (NiCd), nickel-metal hydride (Ni-MH) and sodium-sulphur batteries [9],[24] as shown in figure 1.2. Furthermore, Li ion batteries have shown a proven track record of reliability in the portable electronics market since their introduction in the 1990's [23] and continue to

enjoy great success with a global market size projected to reach USD (United States Dollar) 105.0 billion by 2025 [22].

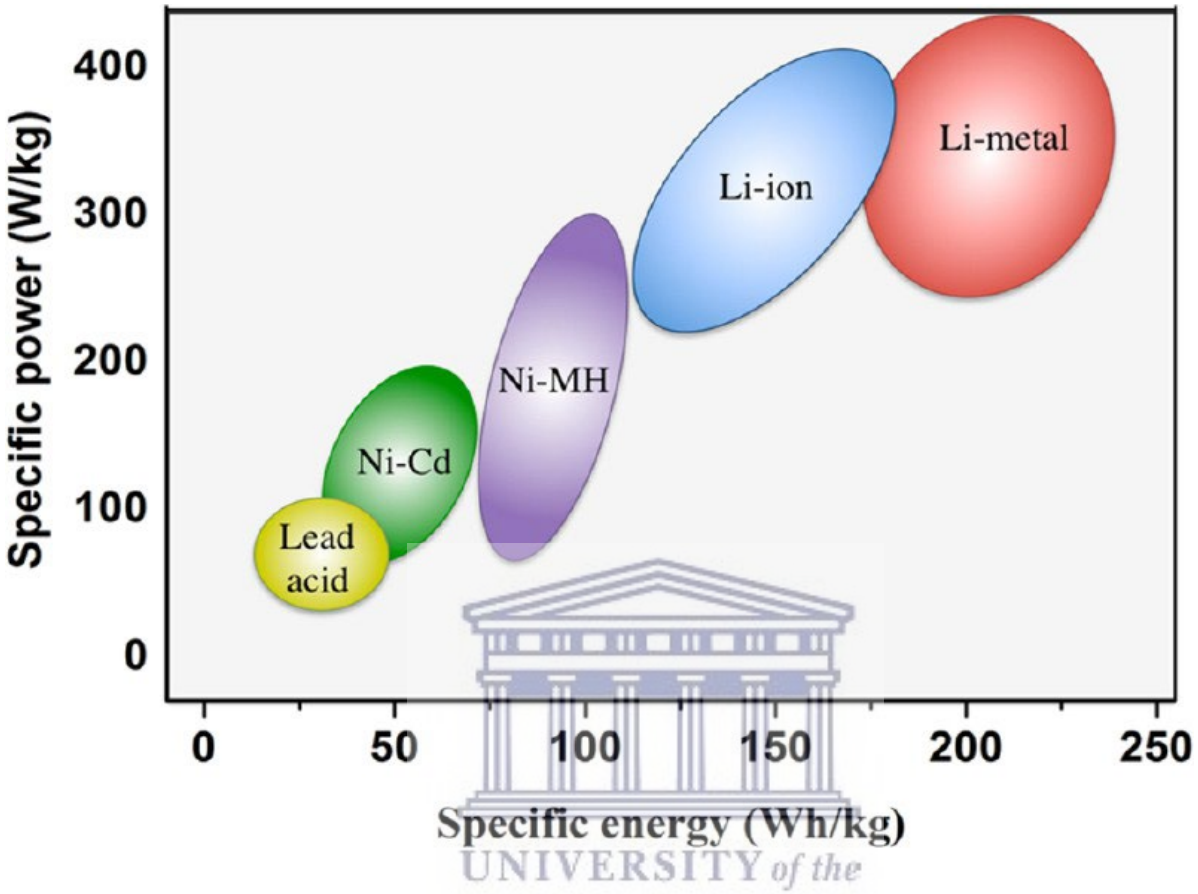

Figure 1.2: Ragone plot of the various battery technologies [9].

However, currently available Li-ion batteries cannot meet all the requirements for applications in electric vehicles and electrical grid storage systems. These include, extended lifespan, low production cost, environmentally benign, high-energy density, and good safety [25]. For example, the best performing commercial Li-ion battery consists of a cobalt based cathode ($LiCoO_2$) which is both costly and toxic [26]. The limiting factor to higher capacity and performance in Li-ion batteries is the relatively low capacities of their cathode materials ($LiCoO_2$, $LiNiO_2$, $LiMn_2O_4$, $LiFePO_4$ and $LiMnO_2$) with specific capacities ranging from 100–180 mA h g^{-1} [27].

This work reports on the use of a novel nanostructured lithium rich manganese oxides (Li_2MnO_3) doped with europium (Eu) and surface coated with Palladium oxide (PdO) composite as high-capacity cathodes for potential grid storage and electric vehicle Li-ion batteries application. This is because of the low cost of manganese due to its

abundance, high theoretical capacities (459 $mAhg^{-1}$) and its low toxicity of the materials.

1.2. Problem Statement

The activation of Li_2MnO_3 cathode materials by the loss of lattice oxygen from the structure during the initial cycling results in the irreversible capacity loss and low initial coulombic efficiencies [28]. This occurs because of the detached lattice oxygen reacting with the electrolyte and decomposing it [28]. Furthermore, this oxygen loss destabilises the [MnO_6] octahedral symmetry and induces a phase transformation where transition metals migrate in favour of a more stable tetrahedral geometry (spinel) according to Jahn Teller distortion [29]. It has been suggested that to supress the capacity fading during cycling, the suppression of oxygen dimerization and phase transformation to spinel must be employed [29]. Herein, we report on the strategies that have been employed to suppress oxygen dimerization and phase transformation to spinel [29].

1.3. Motivation

The fabricated composite yields a synergistic relationship which shortens Li^+ diffusion pathways and improves rate capability. Secondly, surface coating can suppress electrode/electrolyte side reactions and lastly rare earth element (REE) doping which can reduced charge transfer resistance and increase electric conductivity.

1.4. Research Aims & Objectives

1.4.1. Research Aim

The aim of this study was to prepare, characterize and determine the electrochemical attributes of modified Li_2MnO_3 cathode materials for possible Li-ion battery application.

1.4.2. Objectives

1. Prepare Li_2MnO_3, $Li_2Mn_{0.95}Eu_{0.05}O_3$ and $PdO@Li_2Mn_{0.95}Eu_{0.05}O_3$.
2. Perform structural characterization of Li_2MnO_3, $Li_2Mn_{0.95}Eu_{0.05}O_3$ and $PdO@Li_2Mn_{0.95}Eu_{0.05}O_3$.

3. Evaluate the electrochemical performance of Li_2MnO_3, $Li_2Mn_{0.95}Eu_{0.05}O_3$ and $PdO@Li_2Mn_{0.95}Eu_{0.05}O_3$.

References

1. OECD, “Green Growth Indicators 2014”, OECD Green Growth Studies, OECD Publishing., 2014.
2. United Nations, “World population prospects 2019: highlights”, Department of Economic and Social Affairs, Population Division., no. 14,.2019.
3. World Energy Council, “World Energy Scenarios 2019: Exploring Innovation Pathways to 2040”, World Energy Council., 2019.
4. Patade, V.Y., Meher, L.C., Grover, A., Gupta, S.M. and Nasim, M., 2018. Omics Approaches in Biofuel Technologies: Toward Cost Effective, Eco-Friendly, and Renewable Energy*, In Omics Technologies and Bio-Engineering*, pp. 337-351, Academic Press.
5. Eskom, “Electricity generation in South Africa,” The generation of electricity is the conversion of other forms of energy into an electrical current. There are different forms of electricity generation., 2016. [Online]. Available: http://www.eskom.co.za/news/Pages/Nov2.aspx. [Accessed: 11-Feb-2020].
6. World Nuclear Association, “Where does our electricity come from?” [Online]. Available: https://www.world-nuclear.org/nuclear-essentials/where-does-our-electricity-come-from.aspx. [Accessed: 11-Feb-2020].
7. United States Environmental Protection Agency, “Greenhouse Gas Emissions,” Overview of GreenhouseGases. [Online]. Available: https://www.epa.gov/ghgemissions/overview-greenhouse-gases.
8. North, G.R., 2015. Climate and climate change| greenhouse effect. Second Edition., vol. 2. Elsevier, 2015.
9. Ninawe, A.S., Indulkar, S.T. and Amin, A., 2018. Impact of climate change on fisheries. *In Biotechnology for Sustainable Agriculture*, pp. 257-280. Woodhead Publishing.
10. Saroha, R., Panwar, A.K., Gaur, A., Sharma, Y., Kumar, V. and Tyagi, P.K., 2018. Electrochemical studies of novel olivine-layered ($LiFePO_4$-Li_2MnO_3) dual

composite as an alternative cathode material for lithium-ion batteries. *Journal of Solid State Electrochemistry*, 22(8), pp. 2507-2513.

11. Zuo, Y., Li, B., Jiang, N., Chu, W., Zhang, H., Zou, R. and Xia, D., 2018. A high-capacity O_2-type Li-rich cathode material with a single-layer Li_2MnO_3 superstructure. *Advanced materials*, 30(16), p.1707255.
12. Zhao, W., Xiong, L., Xu, Y., Xiao, X., Wang, J. and Ren, Z., 2016. Magnesium substitution to improve the electrochemical performance of layered Li_2MnO_3 positive-electrode material. *Journal of Power Sources*, 330, pp.37-44.
13. Martins, F., Felgueiras, C., Smitkova, M. and Caetano, N., 2019. Analysis of fossil fuel energy consumption and environmental impacts in European countries. *Energies*, 12(6), p.964.
14. Grunwald, A., Wyss, M. and Peppoloni, S., 2015. The imperative of sustainable development: Elements of an ethics of using georesources responsibly. Geoethics ethical challenges and case studies in Earth sciences, pp.25-35.
15. World-nuclear.org. 2021. [online] Available at: <http://www.world-nuclear.org/uploadedFiles/org/WNA/Publications/Working_Group_Reports/comparison_of_lifecycle.pdf> [Accessed 15 February 2021].
16. Longo, M., Yaïci, W. and Foiadelli, F., 2018. 'Electric vehicles integrated with renewable energy sources for sustainable mobility. *New trends in electrical vehicle powertrains*, pp.203-223.
17. Shaheen, S.A. and Lipman, T.E., 2007. Reducing greenhouse emissions and fuel consumption: Sustainable approaches for surface transportation. *IATSS research*, 31(1), pp.6-20.
18. Nieuwenhuis, P., Cipcigan, L. and Sonder, H.B., 2020. The electric vehicle revolution. *In Future Energy*, pp. 227-243. Elsevier.
19. Perner, A. and Vetter, J., 2015. Lithium-ion batteries for hybrid electric vehicles and battery electric vehicles. *In Advances in battery technologies for electric vehicles,* pp. 173-190. Woodhead Publishing.
20. Falk, J., Nedjalkov, A., Angelmahr, M. and Schade, W., 2020. Applying Lithium-Ion Second Life Batteries for Off-Grid Solar Powered System—A Socio-Economic Case Study for Rural Development. *Zeitschrift für Energiewirtschaft*, 44(1), pp.47-60.

21. Vega-Garita, V., Hanif, A., Narayan, N., Ramirez-Elizondo, L. and Bauer, P., 2019. Selecting a suitable battery technology for the photovoltaic battery integrated module. *Journal of Power Sources*, 438, p.227011.
22. Statista. 2021. Projected global lithium-ion battery market size 2025 | Statista. [online] Available at: <https://www.statista.com/statistics/1011187/projected-global-lithium-ion-battery-market-size/> [Accessed 15 February 2021].
23. Placke, T., Kloepsch, R., Dühnen, S. and Winter, M., 2017. Lithium ion, lithium metal, and alternative rechargeable battery technologies: the odyssey for high energy density. *Journal of Solid-State Electrochemistry*, 21(7), pp.1939-1964.
24. Chen, T., Jin, Y., Lv, H., Yang, A., Liu, M., Chen, B., Xie, Y. and Chen, Q., 2020. Applications of lithium-ion batteries in grid-scale energy storage systems. *Transactions of Tianjin University*, 26(3), pp.208-217.
25. Diouf, B. and Pode, R., 2015. Potential of lithium-ion batteries in renewable energy. *Renewable Energy*, 76, pp.375-380.
26. Bazito, F.F. and Torresi, R.M., 2006. Cathodes for lithium ion batteries: the benefits of using nanostructured materials. *Journal of the Brazilian Chemical Society*, 17(4), pp.627-642.
27. Nitta, N., Wu, F., Lee, J.T. and Yushin, G., 2015. Li-ion battery materials: present and future. *Materials today*, 18(5), pp.252-264.
28. Ye, D., Zeng, G., Nogita, K., Ozawa, K., Hankel, M., Searles, D.J. and Wang, L., 2015. Understanding the Origin of Li2MnO3 Activation in Li-Rich Cathode Materials for Lithium-Ion Batteries. *Advanced Functional Materials*, 25(48), pp.7488-7496.
29. H. Chen and M. S. Islam, “Lithium extraction mechanism in Li-rich Li_2MnO_3 involving oxygen hole formation and dimerization,” *Chemical Materials*, vol. 28, no. 18, pp. 6656–6663, 2016.

CHAPTER 2

LITERATURE REVIEW

2.1. Literature Review

2.1.1. History of Li-ion batterie

Investigations into Li-ion based batteries began as early as the 1970's [1]. This was after the discovery that a Li-ion has the smallest radius in contrast with all the metals and can move reversibly between two interacted materials of different potentials when used as electrodes [1],[2]. This concept was quickly taken up and implemented by M.S Whittingham to produce a battery with lithium metal as an anode and titanium disulphide (TiS_2) as a cathode [2]. Although these types of batteries showed great promise with high energy densities, they had an inherent flaw in that the lithium metal anode exhibited uneven dendritic growth during cycling which ultimately raised safety concerns as depicted in figure 2.1 [2].

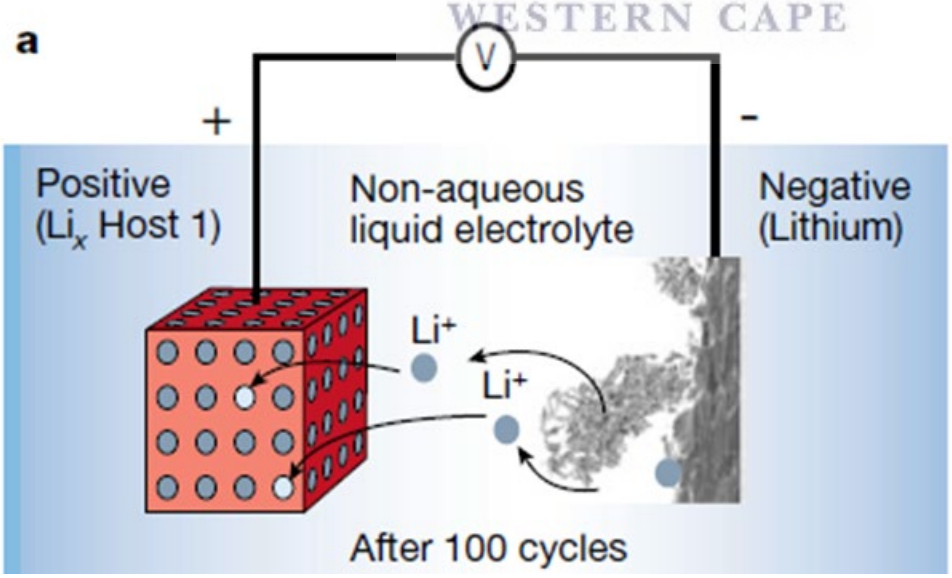

Figure 2.1: Schematic diagram of an early Li-ion battery showing Li dendrite growth on anode [4].

As a result of the mounting safety concerns of lithium metal anodes, a few alternative anodes where proposed. The newly proposed anodes were fabricated by alloying lithium with other metals, examples of such anodes included Li/AL and Li/Mn [1],[3]. The lithium alloy anodes lowered the rate of lithium dendritic growth but in the process compromised the electrode potential and capacity of the battery [3]. This prompted Goodenough in the 1980's to investigate new cathode materials with high voltages which he found to be layered lithiated transition metal oxide of the formula $LiMO_2$ (where M= Co, Ni, Cr & V) [1],[2],[3]. Goodenough's discovery together with the discovery of the highly reversible, low voltage Li intercalation–deintercalation process in carbonaceous material paved the way for the world's first commercial rechargeable battery by SONY corporation in 1991 [2],[4],[7].

2.1.2. Working principle of Li-ion batteries

The working principle of rechargeable Li-ion battery is based on the ability of the lithium ions to move reversibly between the anode and cathode of a cell during charging and discharging as depicted in figure 2.2 [5],[7]. During the charging process, lithium ions intercalate into the carbonaceous intercalated anode (graphite) from the lithiated metal oxide cathode ($LiMO_2$ where M= Co, Mn, Cr or V) [5],[6]. During the discharging process, lithium ions intercalate back into the lithiated metal oxide cathode from the carbonaceous intercalated anode (graphite) and this movement of the lithium is generating a flow of electrons through an external circuit [5],[7]. This process can be summarized the equations (2.1 - 2.3) below [6]:

Cathode: $LiCoO_2 \leftrightarrow Li_{1-n}CoO_2 + nLi^+ + ne^-$ (2.1)

Anode: $C_6 + nLi^+ + ne^- \leftrightarrow Li_nC_6$ (2.2)

Cell reaction: $LiCoO_2 + C_6 \leftrightarrow Li_nC_6 + Li_{1-n}CoO_2$, E_o = ~ 4 V (2.3)

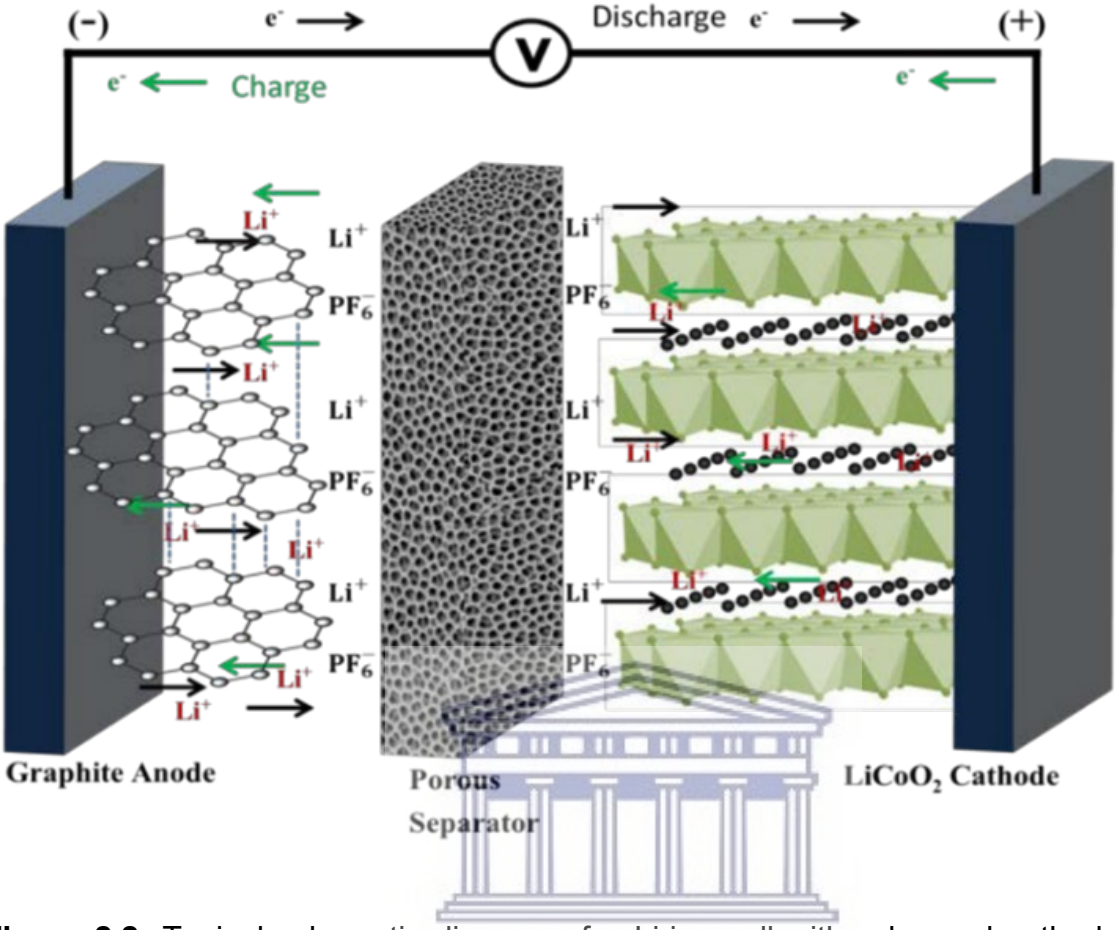

Figure 2.2: Typical schematic diagram of a Li-ion cell with a layered cathode and graphitic anode [6].

2.1.3. Components of Li-Ion Batteries

2.1.3.1. Electrolyte

An electrolyte is an important component of a cell that is localized between the electrodes of a cell. It is responsible for the migration of ions between the two electrodes of the cell which is associated with ionic charge transport [11]. Two types of electrolytes for Li-ion batteries exist, liquid electrolytes and solid type electrolytes. The most common type of electrolytes used to date are liquid electrolytes. Examples include lithium hexafluorophosphate ($LiPF_6$), lithium perchlorate ($LiClO_4$) or lithium tetrafluoroborate ($LiBF_4$) [11]. The choice of the electrolyte used in a cell determines the electrochemical window of the cell. The electrochemical window of a cell is a voltage range in which the electrolyte will neither be oxidized or reduced. Properties of an ideal electrolyte are [8],[9]:

- Chemically stable/inert (non-reactive with electrodes and other cell components)
- High ionic conductivity
- Resistant to change in harsh conditions (thermal & mechanical)
- Large electrochemical window ~5 V vs Li^+/Li.

2.1.3.2. **Anode**

The anode is a negative electrode within the cell at which the process of oxidation takes place, and an electron is released into the external circuit. In Li-ion batteries, lithium metal was found to be the best anode but was quickly replaced by carbonaceous intercalated materials due to safety concerns associated with the uneven dendritic growth during cycling. An ideal electrode must have strong reducing ability, be able to undergo lithium intercalation/deintercalation processes rapidly, have good conductivity and a low cost [12].

2.1.3.3. **Separator**

The separator is put in place within a cell to prevent electronic contact of the two electrodes and to allow free migration of ions from one electrode to another. Typically, separators are fabricated from Polyolefins, natural and/or synthetic fibres (non-woven separators) and ultrafine metal oxide or carbonate particles (inorganic composite separators) [11]. Ideal properties of separators include [11]:

- Chemical stability.
- A relative thickness that will exhibit porosity < 1mm.
- Uniform permeability.

2.1.3.4. **Cathode**

In Li-ion batteries, the physico-chemical properties of the battery are directly dependent on the type of the cathode and anode materials used [14], [17], [18]. These properties subsequently have a greater influence on the performance and the overall cost of the battery [19]. For example, the cathode material used in commercial Li-ion batteries such as $LiCoO_2$, Li_2MnO_4 and $LiFePO_4$ have specific capacities of 100~180 $mAh.g^{-1}$ which are significantly lower as compared to the anode material graphite

which has a specific capacity of ~373 mAh.g^{-1} [20]. This implies that in order to significantly improve battery performance, the cathode materials become the first component to fine tune because it has a lower specific capacity compared to the anode and the Li-ion transfer when charging and discharging is mainly controlled by the cathode [17],[19].

One family of cathode materials that has generated worldwide interest for Li-ion battery application in electric vehicles, hybrid vehicles and off grid storage is the lithium manganese oxides[21]. This is a result of the low cost of manganese due to its abundance, high theoretical capacities, and the low toxicity of the materials [21]. One such material is the lithium manganese oxide Li_2MnO_3 which possesses a superior theoretical capacity of 459 mAh.g^{-1}[22].

Due to its insulator-like properties, Li_2MnO_3 was thought to be electrochemically inactive [23],[24]. It was in 1991 when Thackeray *et al*. [25] at the CSIR discovered that a new type of electrochemically active layered oxide could be produced by simply leaching out LiO_2 from Li_2MnO_3 by acid treatment at room temperature. When electrochemically cycled, they obtained $0.2Li_2MnO_30.8LiMnO_2$ layered material which ushered the dawn of a new Li_2MnO_3 based layered-layered cathode materials and the notation $xLi_2MnO_3(1-x)LiMnO_2$ [25].

In another study, it was reported that Li_2MnO_3 could also be activated electrochemically by charging to >4.5 V [25]. These lithium rich manganese oxides (LRMOs) possess specific capacities of up to 280 mAh.g^{-1} [25]. It has been proposed that the Li_2MnO_3 component stabilizes the structure at lower voltage regions and can also provide addition lithium ions in the high voltage region [25]. Nevertheless, the large-scale application of these LRMOs cathode materials remained limited due to cut-off voltage for activation, irreversible capacity loss in the first cycle and transition metal migration which induces phase transformation during repeated charge-discharge cycles which have been attributed to the Li_2MnO_3 component [25], [26].

As a result of the factors discussed above, it becomes imperative to investigate ways to improve the electrochemical properties of Li_2MnO_3 to fabricate higher capacity Li_2MnO_3 and LMRO cathodes. This review presents research advances in the modification of Li_2MnO_3 to suppress irreversible capacity loss and improve capacities.

It further presents 1st principle studies of proposed modifications for high capacity Li_2MnO_3 derivatives as well as reported experimental work. Furthermore, it discusses in depth the modification strategies such as Mn-ion substitution, surface coating, surface treatment, combined modifications, and alternative phase embedment. Finally, it also explores the significance of these Li_2MnO_3 modifications, and the effectiveness of these modification techniques are also being compared.

2.1.3.4.1. Li_2MnO_3 structure and electrochemical activity origin

The layered manganese oxide Li_2MnO_3 can be expressed as $Li[Li_{0.33}Mn_{0.66}]O_2$, indicating that it possesses an α-$NaFeO_2$ type structure with the space group of $C2\backslash m$ monoclinic [20],[27]. In this structure, alternating lithium, close cubic packed oxygen, and transition metal layers are stacked one on the other in an ABCABC stacking order as represented in figure 2.3. From the notation $Li[Li_{1/3}Mn_{2/3}]O_2$, it becomes evident that 1/3 of the inter-slab octahedral sites are occupied by Li^+ and the remaining 2/3 by Mn^{4+}. In other words, 1/3 of the Mn^{4+} in the transition metal (TM) layer are replaced by Li^+ [23],[28]. As a result of this occupancy of Li^+ in the TM layer, a honeycomb configuration consisting of 6 Mn^{4+} surrounding 1 Li^+ exists and can be observed as a superlattice using X-ray diffraction (XRD) as shown in figure 2.4 [20],[27],[29]. This super lattice is characteristic of Li_2MnO_3 materials and can be observed using XRD (figure 2.4) at 20 – 25° 2θ angles [30],[31].

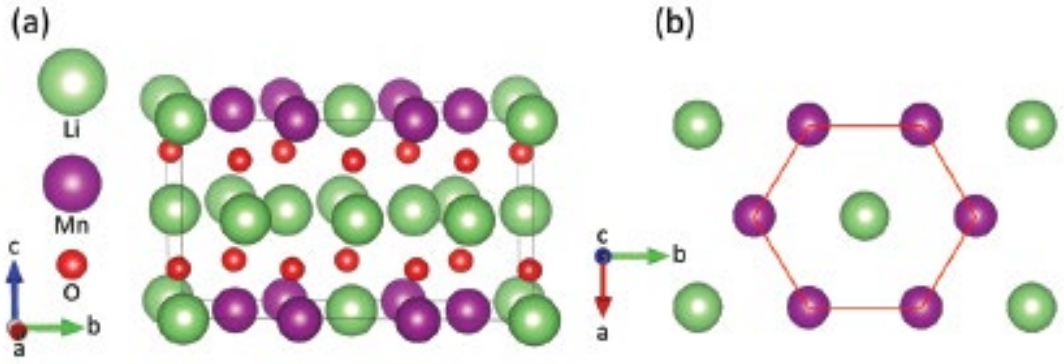

Figure 2.3:(a)Schematic representation of the crystallographic structure of Li_2MnO_3 (b) Honeycomb configuration of 6 Mn^{4+} surrounding 1 Li^+ in the TM layer of Li_2MnO_3 [28].

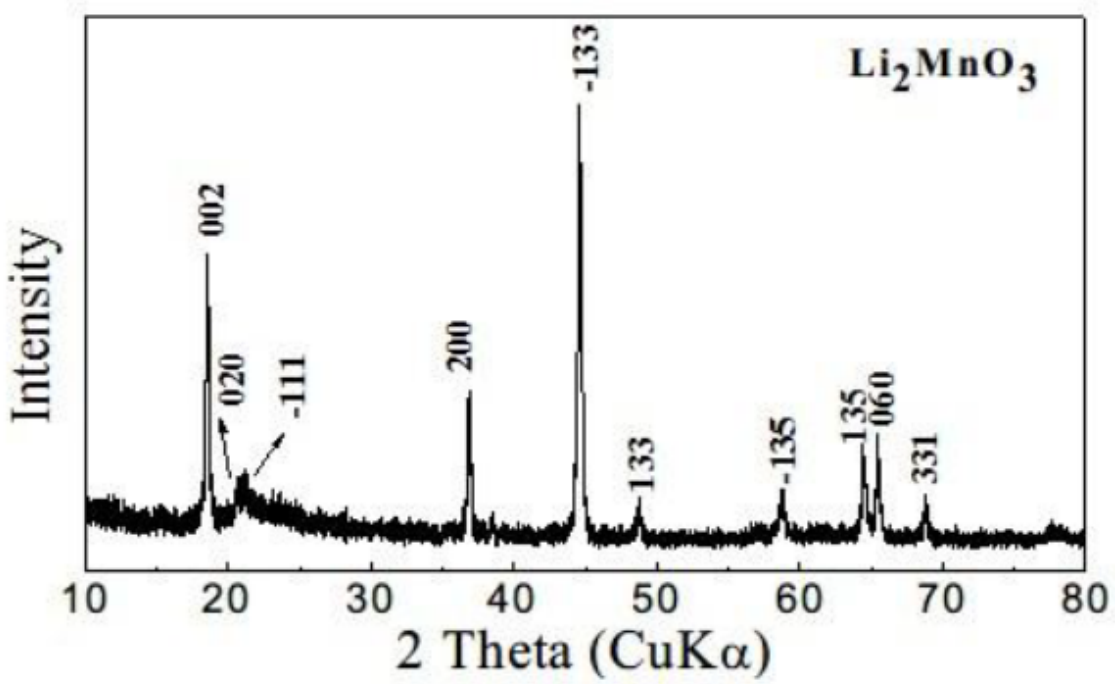

Figure 2.4: XRD pattern of monoclinic Li_2MnO_3 [27].

It is generally accepted that in lithiated manganese oxide cathode materials such as $LiMnO_2$ and $LiMn_2O_4$, the electrochemical activity is associated with Li^+ intercalation and deintercalation which is accompanied by the oxidation of manganese from Mn^{3+} to Mn^{4+} [24]. Thus, for a very long time Li_2MnO_3 was thought to be electrochemically inactive due to Mn^{4+} being unable to oxidize to higher state of Mn^{5+}. Today it is well established that Li^+ ions can successfully be deintercalated and intercalated back into this material, although the origin of the electrochemical activity of Li_2MnO_3 is still a highly debatable subject.

The origin of the electrochemical activity of Li_2MnO_3 is still highly debatable, complex in nature and yet to be fully understood. Initially, the charge compensation in Li_2MnO_3 was attributed to the O losing electrons in order to achieve charge neutrality during the first charge (>4.5 V vs Li/Li^+). The proposed equation 2.4 was given as:

$$Li_2MnO_3 \rightarrow Li_2O + MnO_2 \quad (2.4)$$

Robertson *et al*. [24] did an extensive study on the electrochemical activity of Li_2MnO_3 and suggested that the activity could be attributed more to the ion exchange between the H^+ proton from the electrolyte and Li^+ ion from Li_2MnO_3. Similar results were observed even in anhydrous organic electrolytes such as $LiPF_6$ which have been known to produce hydrogen fluoride (HF) when interacting with even small volumes of water [24]. From this work, it was concluded that the mechanism in Li_2MnO_3 electrochemical activity is the compensation of charge between Li^+ and H^+ as opposed to the loss of O^{2-}. This conclusion was backed by flame emission spectroscopy (FES), atomic absorption spectroscopy (AAS), X-ray photoelectron spectroscopy (XPS) and thermogravimetric analysis/mass spectroscopy (TGA/MS) results of the sample measured during charge and discharge as shown in table 2.1.

Table 2.1: FES, AAS, XPS and TGA/MS results of the sample measured during charge and discharge [24].

Sample	Calculated Li:Mn ratio	Theoretical Li:Mn ratio	Calculated H	Bulk Composition
1st charge 55°C	$Li_{0.62}Mn$	$Li_{0.65}Mn$	$H_{1.29}$	$Li_{0.62}H_{1.29}MnO_{2.95}$
1st discharge 55°C	$Li_{1.28}Mn$	$Li_{0.65}Mn$	$H_{0.66}$	$Li_{1.29}H_{0.66}MnO_{2.97}$

From the first charge, the electrolyte undergoes oxidation to generate H^+ protons which undergo ion exchange with Li^+ ions derived from the electrode surface. This implies that H^+ protons now coexist with Li^+ ions within the structure of the material. Upon first discharge, the electrolyte reduction process drives the extraction of the H^+ protons from the structure and Li^+ ions are intercalated back into the structure. From the table above it can be observed that the loss of oxygen is minimal and thus cannot be the dominant mechanism in the electrochemical activity of Li_2MnO_3.

Although there is significant evidence for the Li^+/H^+ ion exchange mechanism during electrochemical cycling, some reports dispute this being the main mechanism for the activity of Li_2MnO_3 [32],[33]. It is suggested that this mechanism is dominant at elevated temperatures where electrode degradation can take place [32]. Yu *et al*. [32] reported that during the de-lithiation process at room temperature, oxygen gas is generated, accounting for ~1/8 moles from $Li[Li_{1/3}Mn_{2/3}]O_2$ thus further reinforcing the

oxygen loss hypothesis. Chen *et al*. [33] supported the oxygen loss mechanism by suggesting that Li extraction is accompanied by oxygen loss which generates holes on oxygen. These holes are not stable and are stabilized by the formation of molecular oxygen which facilitates the migration of Mn ions onto vacant octahedral sites in the lithium layers and generates a spinel type material [33]. The equation and mechanism supporting the observation are given in equation 2.5 and figure 2.5 respectively.

$Li_2MnO_3 \rightarrow 2Li^+ + 2e^- + MnO_2 + O_2$ (2.5)

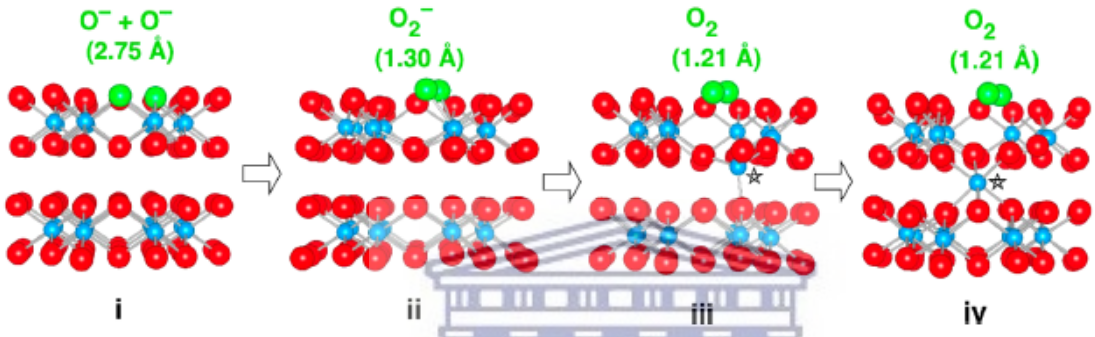

Figure 2.5: Oxygen loss mechanism suggesting that Li extraction is accompanied by oxygen loss which generates holes on oxygen which result in oxygen evolution [33].

2.1.3.4.2. Challenges facing Li_2MnO_3 as cathode materials

The activation of Li_2MnO_3 cathode materials by the loss of lattice oxygen from the structure during the initial cycling results in the irreversible capacity loss and low initial coulombic efficiencies [27],[28],[29]. This occurs as a result of the decomposition of the detached lattice oxygen through its reaction with the electrolyte. Furthermore, this oxygen loss destabilizes the [MnO_6] octahedral symmetry and induces a phase transformation where transition metals migrate in favour of a more stable tetrahedral geometry (spinel) in accordance with Jahn Teller distortion [28]. It has been suggested that in order to minimize capacity fading during cycling, approaches related to the suppression of oxygen dimerization and phase transformation to spinel must be carried out. Herein, we report on such strategies.

2.1.3.4.3. Li_2MnO_3 Modification Strategies

2.1.3.4.3.1. Particle Size Confinement

Nanoscale confinement has been reported to significantly enhance the thermodynamic and kinetic properties of Li-ion cathode materials [34]. Nanostructures have shorter Li^+ diffusion pathways which can improve the rate capability during Li ion intercalation/de-intercalation processes [35], [36]. Shortened diffusion pathways offer high power density and reduces the time it takes to reach active sites, resulting in enhanced reaction kinetics [36]. On the other hand, nanostructures (table 2.2) exhibit large specific surface areas which can expose more active sites thus increasing contact between the electrode material and electrolyte leading to greatly improved capacities of the cathode material [37],[38]. Moreover, nanostructures have more defects which can lead to enhanced stability of the structure during cycling and decrease potential barriers [28],[29],[37]. The above-mentioned improvements can be observed in table 2.2, which shows a comparison of the different improvements observed by the nano structuring process using different synthesis approaches.

Table 2.2: Comparison of different Li_2MnO_3 nanostructures and their enhancements.

Morphology	Synthesis Method	Initial Discharge Capacity ($mAh.g^{-1}$)	Initial Coulombic efficiency (%)	Retained Capacity ($mAh.g^{-1}$)	Rate Capacity ($mAh.g^{-1}$)	Particle Size (nm)	Measurement Conditions	Ref.
Nanoparticles & Nano cubes Mix	Solid state	335	100	291	245 (46 mA. g^{-1})	10	2.1- 4.4 V, 11.5 mA. g^{-1}, 3 cycles, RT	[39]
	Hydrothermal	323	70	~187.5	-	10-50	2.0 - 4.3 V, 60mA.g^{-1}, 20 cycles, RT	[27]
Nanoparticles	Solid state	241.9	75.4	182.39	187.23(0.2C)	10-20	2.0-4.6V, 0.1C, 45 cycles, RT	[40]
	Oxidation reaction	236	78.15	~187.5	100 (914.3mA.g^{-1})	~10	2.0-4.9V ,14.3 mA. g^{-1}, 30 cycles, RT	[41]
	Sol gel	173	-	~105	-	10~40	2.0-4.6 V, 30 cycles, RT	[42]
	Solid state	124.9	-	106.2	80.4 (1/20C)	30-80	2.0-4.6V, 100 cycles, 10mA.g^{-1}, RT	[30]
Nanowires	Molten salt	~156	-	159.8	~200 (0.04C)	10-25	2.0 - 4.8 V, 20 mA. g^{-1}, 27 cycles, RT	[43]
	Solid State	~80	~50	~110	100(5C)	50	2.0-4.5V, 100 cycles	[44]
Nanoplate	Precipitation	94	-	82	-	~15	2.0 - 4.8 V, 50 cycles, RT	[45]
Nanoribbon	Ion exchange and oxidation	74	52.11	125	-		2.0 – 4.8 V, 10 mA·g^{-1}, 6 Cycles, RT	[46]
Nanobelts	Ion exchange and oxidation	61.2	33.6	~74	-	15	2.0–4.8 V, 200 mA·g^{-1}, 30 Cycles, RT	[29]

For instance, Liu *et al*. [27] prepared nanostructured Li_2MnO_3 particles by self-seeding hydrothermal methods and obtained well crystallized nanorods and nano cubes with a size range of 10-50 nm as can be observed in figure 2.6 (a). The nanostructures exhibited an initial discharge capacity of 323 $mAh.g^{-1}$ and a specific capacity of 243 $mAh.g^{-1}$ within the voltage window 2.0-4.3 V. In another study, the molten-salt method was used to synthesize Li_2MnO_3 nanowires (figure 2.6 (b)) from Mn_2O_3 nanowire precursor [43]. The nanowires showed an initial discharge capacity of 156 $mAh.g^{-1}$ compared to 53 $mAh.g^{-1}$ from the bulk Li_2MnO_3 in the potential window 2.0 to 4.8 V and current density of 20 $mAh.g^{-1}$ [43]. After 27 cycles, the nanowires retained a discharge capacity of 159.8 $mAh.g^{-1}$. In both studies, the exceptional capacities are attributed to shorter Li^+ diffusion pathways and high surface areas which exposed more particles to the electrolyte leading to a lower activation potential.

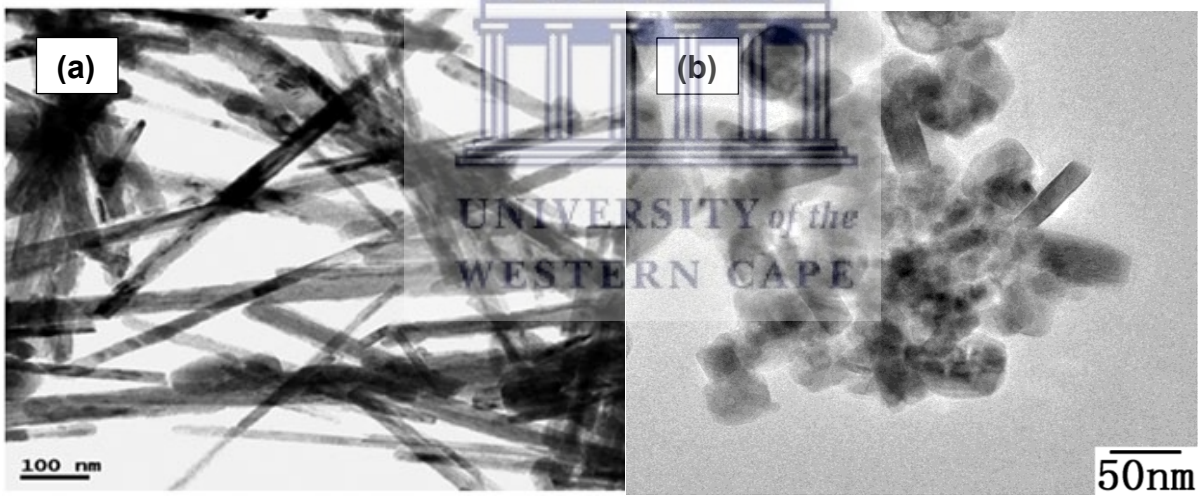

Figure 2.6: TEM images of (a) Li_2MnO_3 Nanowires and (b) Li_2MnO_3 Nanorods and nano cubes [27] [43].

Freire *et al*. [39] reported on nanostructured Li_2MnO_3 obtained by solid state reaction of Li_2O and MnO_2 followed by high energetic grinding at 700 rpm for 20 hours. From TEM studies, the average crystallite size was found to be 10nm in diameter indicating that the material was nanostructured [39]. The initial discharge capacity exhibited was 335 $mAh.g^{-1}$ with no observed drop in capacity during discharge in the potential window 1.2 – 4.4 V vs Li^+/Li at C/40. After 3 cycles, the material showed a reversible

capacity of 291 mAh.g^{-1} and a potential of 3 V at C/40 [39]. More interestingly, even at higher rates, the material still exhibited exceptionally high discharge capacities indicating good cycling stability. The authors attributed the high capacity to the first oxidation process (charging to 4.4 V) which induced disordering in the material.

HRTEM analysis (figure 2.7) of the sample after initial cycling indicated a phase transformation from monoclinic Li_2MnO_3 to a disordered nanostructured material [39]. Most of the sample now contained disordered nano-sized cubic crystals along with traces of pristine monoclinic Li_2MnO_3. It is understood that this transformation to nano-sized cubic crystals improved Li ion diffusion paths.

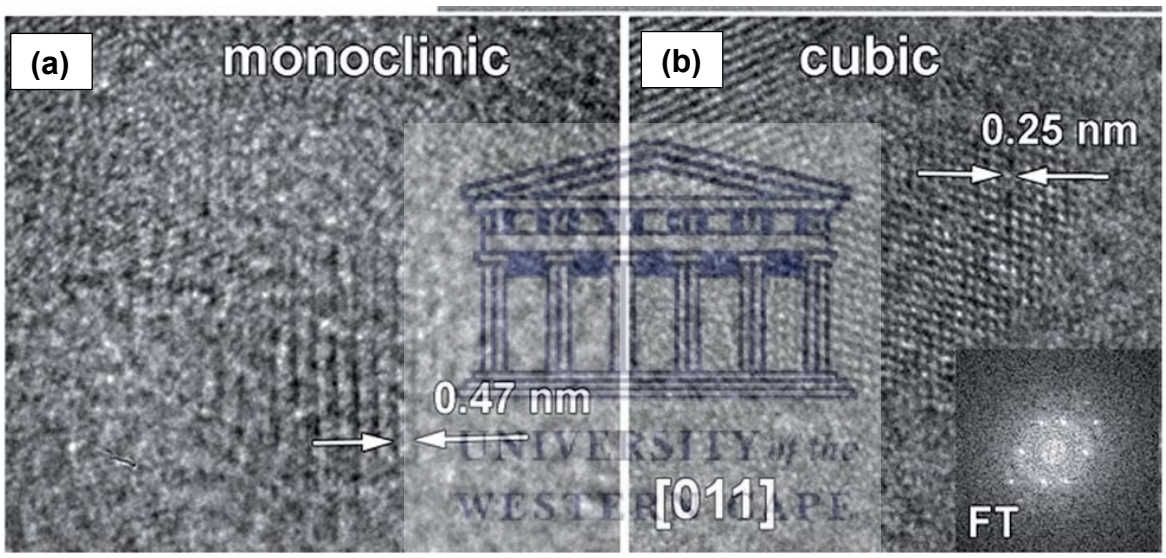

Figure 2.7: HRTEM images of a) single monoclinic and b) cubic nanoparticles [39].

Sayle and co-workers [37] in their 2015 study suggested that the enhancement of electrochemical activity of nanostructured Li_2MnO_3 may also originate from the stabilisation via 'point defect scaffold as shown in figure 2.8. From their Molecular Dynamics simulations, it was determined that the nanostructured Li_2MnO_3 had a high degree of defects and exhibited Li, Mn, and O vacancies with a mix of Li and Mn in all layers (figure 2.8). Unlike in the bulk Li_2MnO_3 which consists of alternating Li ion and transition metal layers, the nanostructured Li_2MnO_3 contained transition metal layers which are held apart by Mn ions (point defects) in the Li ion layer. This Mn ions stabilise the structure of the material during deintercalation thus preventing structural collapse and allowing the smooth diffusion of Li ion in and out of the structure.

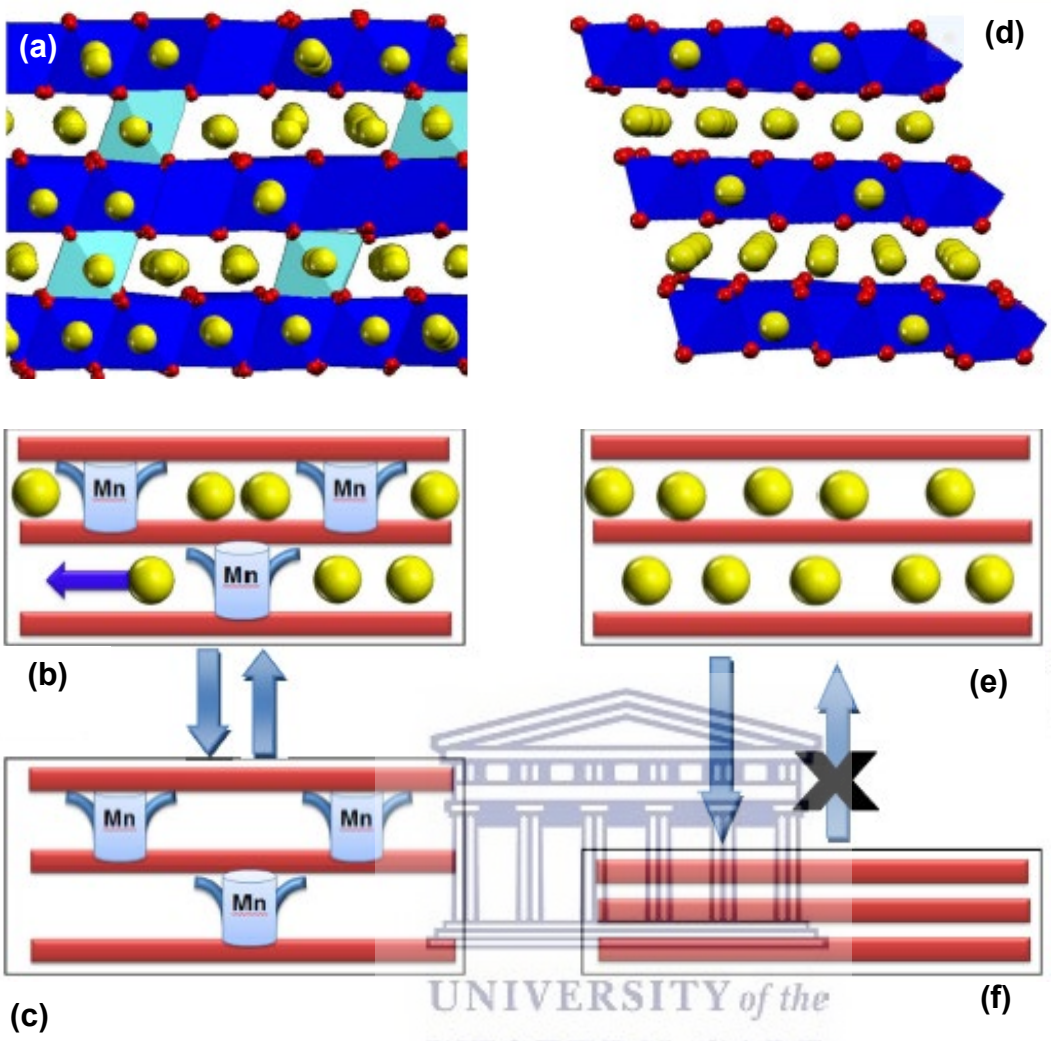

Figure 2.8: Model structures of the proposed stabilization by point defect scaffold [37].

From table 2.2, it is evident that the synthesis method and conditions also play a pivotal role in the electrochemical performances of the nanostructured materials. The synthesis method determines the number of defects (staking faults, Li, Mn or O vacancies and cationic site mixing) which are reported to improve performance of the cathode material [29],[37]. Menon *et al*. [47] reported a similar finding when he compared solid state and sol gel synthesized Li_2MnO_3. Sol gel synthesized Li_2MnO_3 contained more staking faults and exhibited a superior performance compared to the solid-state counterparts [47]. An enhanced performance due to Li and Mn cationic mixing and defects was also observed by Matsunaga *et al*. [48] in their report, where a low synthesis temperature induced Li/Mn cation mixing defects which promoted the smooth diffusion of Li ions.

Table 2.3: Comparison of different coating materials and their enhancements.

Class of Coating	Coating	Initial Discharge Capacity ($mAh.g^{-1}$)	Initial Coulombic Efficiency (%)	Retained Capacity after cycling ($mAh.g^{-1}$)	Rate Capacity ($mAh.g^{-1}$)	Measurement Conditions	Ref.
Metal Oxide	TiO_2	Down from 212.3 to 206.8	Maintained at 100	Up from 81.4 to 99.5	Up from 56.54 to 99.56 (100 mA. g^{-1})	2.1- 4.4 V, 20mA.g^{-1}, 100 cycles, RT	[39]
	Co_3O_4	Up from 85 to 178	Up from 60.28 to 97.27	Up from ~40 to 135	-	2.0 – 4.8 V, 10mA.g^{-1}, 50 cycles, RT	[52]
Phosphate Coating	$FePO_4$	Up from 94 to 180	Up from 45.19 to 91	Up from 82 to 175	-	2.0 and 4.8 V, 10mA.g^{-1}, 50 cycles, RT	[45]
Carbonaceous material	Sucrose derived Carbon	Up from 229.1 to 280.5			Up from 51.8 to 117.5 (400 mA. g^{-})	2.0 - 4.8 V, 10 mA. g^{-1}, 27 cycles, RT	[51]
	PVP derived Graphitic Carbon	Down from 239.3 to 206	Up from 59.3 to 61.9	Up from 126.5 to 196.3	Up from 0.3 to 111 (100 mA. g^{-})	2.0 – 4.8 V, 20 mA. g^{-1}, 10 cycles, RT	[53]
Active Cathode Material	$LiCoO_2$	Up from 74 to 180	Up from 52.11 to 72	Up from ~ 110 to 180	-	2.0 - 4.8 V, 10 mA. g^{-1}, 30 cycles, RT	[46]

2.1.3.4.3.2. Surface Coating

Surface coating is one of the most common methods of improving the electrochemical performance of layered manganese oxide cathode materials [49],[50],[51]. Table 2.3 summarizes some of the reported improvement in the electrochemical performance of layered manganese oxides using different coating materials. Oxygen loss and transition metal dissolution occur at the surface of the electrode and thus a suitable coating improves the performance by providing a protective layer which suppresses side reactions between the electrode and the electrolytes as well as prevents migration and dissolution of transition metals [45],[49],[50]. Furthermore, some coatings can react with the surface of the cathode to provide an active layer which improves capacity and stability [45]. When considering surface coatings, it is important to also note that the thickness of the coating plays a crucial role. In a coating such as TiO_2, the increase in TiO_2 thickness correlates with the formation of a Li_xTiO_2 species, which exhibits poor electrical conductivity and leads to decreasing discharge capacities [39]. On the other hand, $FePO_4$ is a direct opposite of this observation. Li_2MnO_3 coated with increased amounts of $FePO_4$ shows an increase in discharge capacities since it can produce Li_xFePO_4 which is electrochemically active [45]. In the case of carbon coatings, a thin coating is desirable as carbon coating induced the formation of Mn^{3+} which helped promote electron transport [50]. Thick coating led to high Mn^{3+} concentrations, which compromise the stability of the material [51].

Metal Oxide Coating

Kim *et al*. [52] synthesized pristine Li_2MnO_3 via sol gel method and proceeded to coat the resulting Li_2MnO_3 with anatase (TiO_2) to form a shell of controlled thickness as shown in figure 2.9. In order to obtain the optimum TiO_2 ratios, oxide coating variations from 4.8 -13.3 wt.% were investigated. The rationale behind TiO_2 as a coating material was based on the difficulty of TiO_2 in reacting with the electrolyte at room temperature according to equation 2.5:

$$TiO_2 + 6HF + 2e^- \rightarrow H_2TiF_6 + 2H_2O \qquad (2.5)$$

From their results, it was found that the coating had no enhancement effect on the initial cycling capacity but rather the initial discharge capacity of the material diminished with increasing TiO_2 content and was attributed to the thickness of the coating. Nonetheless, the coated samples showed an improved cycling stability after 100 cycles. The best performing sample showed a discharge capacity of 125.2 $mAh.g^{-1}$ with a capacity retention of 66.3% as compared to 81.4 mAh g^{-1} at 38.3% shown by uncoated Li_2MnO_3 [52]. In this case, the coating prevented side reactions at the electrode/electrolyte interface as well as Mn dissolution into the electrolyte.

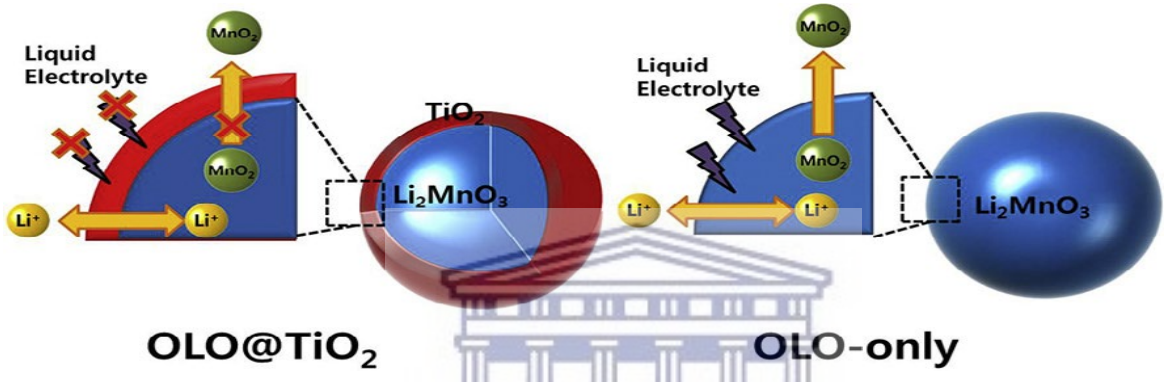

Figure 2.9: An illustration of how a surface coating such TiO_2 affects Li_2MnO_3 [54].

Phosphate Coating

In certain instances, some surface coating materials can improve both the cycling stability and the initial cycle discharge capacity. Such a behaviour was observed when Wang *et al.* [45] produced a core-shell type nanocomposite which consisted of a Li_2MnO_3 nanoplate coated with $FePO_4$. In their report, it was observed that the coating improved the cycling stability as no significant capacity fading was observed in the coated Li_2MnO_3 nanoplate with cycling. The $FePO_4$ coating thus prevented electrode corrosion via side reactions at the electrode/electrolyte interface. As opposed to the TiO_2 coating reported by Kim *et al*. [45] which is an "inert" coating, the $FePO_4$ coating also acted as an active layer which diminished 1st cycle capacity loss and had a specific capacity of 180 $mAh.g^{-1}$ (figure 2.10).

Moreover, the $FePO_4$ coating doubled as a Li-ion host for Li ions that cannot be reinserted into the Li_2MnO_3 and thus exhibited a superior initial cycle discharge capacity of 208 $mAh.g^{-1}$ as shown in figure 2.10. The intercalation of Li ions into the

$FePO_4$ was evidenced by the presence of a reversible redox peak at 2.7/3.0 V vs. Li^+/Li which did not occur in the uncoated counterpart. It is also suggested that small amounts of Fe^{3+} from $FePO_4$ might have been incorporated into the Li_2MnO_3 structure further improving its capacity. Although the suppression of electrode corrosion and the lowered charge transfer resistance can be attributed to surface coating, the nanoscale confinement effect must not be ignored.

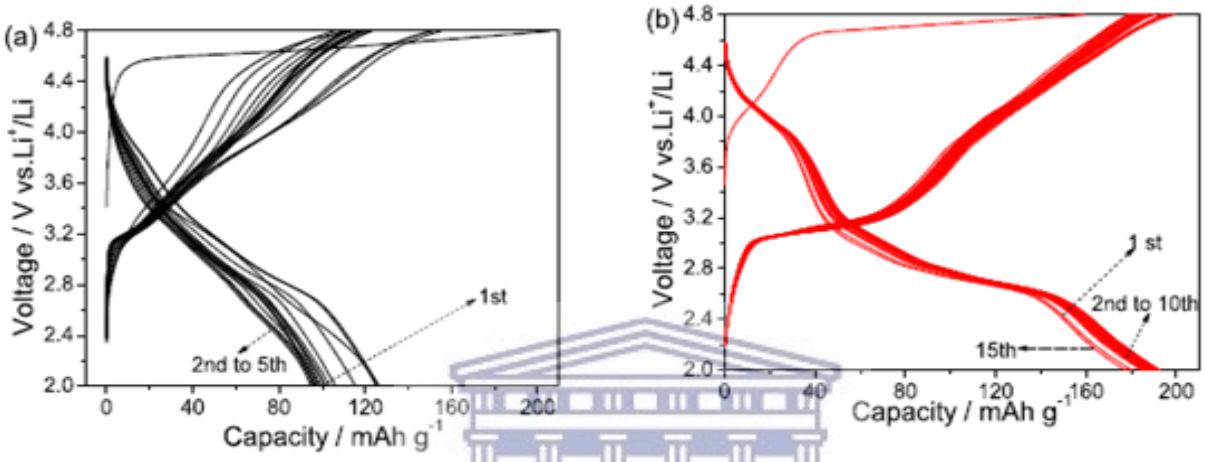

Figure 2.10: Charge/discharge curves of Li_2MnO_3 nanoplates (a) and Li_2MnO_3@$FePO_4$ nanoplates [45].

Carbon coating

Surface coating with carbon & carbonaceous materials has its merits as a low-cost method of improving cathode material performance as they possess excellent conductivity [40],[55],[56]. In one publication by Xiong *et al.* [51], Li_2MnO_3 was produced by solid state reaction of Li_2CO_3 and $MnCO_3$ followed by calcination in air at 500 °C for 4 hours. The obtained powders were mixed with sucrose in ethanol and water while stirring, dried and then calcined at 350 °C for 20, 40 and 60 minutes, respectively [55]. When electrochemical studies were carried out, the carbon coating had a significant effect on the initial cycle discharge capacity of the Li_2MnO_3 and on the rate capacity. The best performing sample delivered a discharge capacity of 280.5 $mAh.g^{-1}$ and 117.5 $mAh.g^{-1}$ at 10 $mA.g^{-1}$ and 400 $mA.g^{-1}$ current densities respectively as shown in figure 2.11 [55]. The pristine sample on the other hand delivered lower capacities of 229.1 $mAh.g^{-1}$ and 51.8 $mAh.g^{-1}$ at 10 $mA.g^{-1}$ and 400 $mA.g^{-1}$ current densities respectively [55]. The high conductivity of the carbon

infrastructure on the surface of Li_2MnO_3 enhanced the electron pathway thus reducing charge transfer resistance.

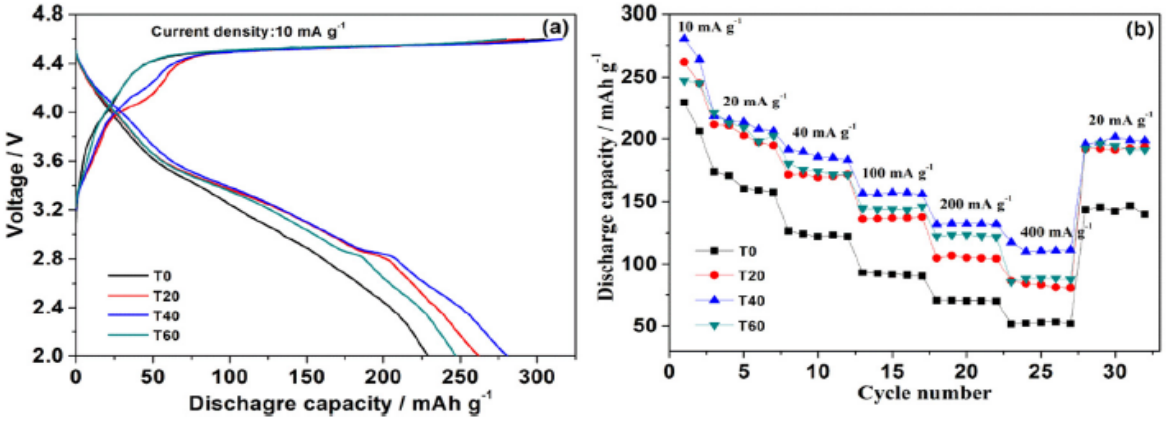

Figure 2.11: (a) Charge/discharge curves of Li_2MnO_3 and various Li_2MnO_3@C samples (b)Cycling stability testing of Li_2MnO_3 and various Li_2MnO_3@C samples [55].

Active cathode material coating

Wang *et al*. [46] produced coaxial $LiCoO_2$@Li_2MnO_3 nanoribbons which exhibited initial charge and discharge capacities of 270 mAh.g^{-1} and 180 mAh.g^{-1} respectively. Even after 30 cycles, the material was able to retain a 180 mAh.g^{-1}, discharge capacity in the potential window 2.0 - 4.8 V vs Li^+/Li as shown in figure 2.12 (b). The exceptional performance was attributed to the $LiCoO_2$ coating which provided additional Li^+ during insertion, suppressed active material corrosion and to the redox couple $Co^{3+/}Co^{4+}$shown in figure 2.12 (a) which can increase the energy density.

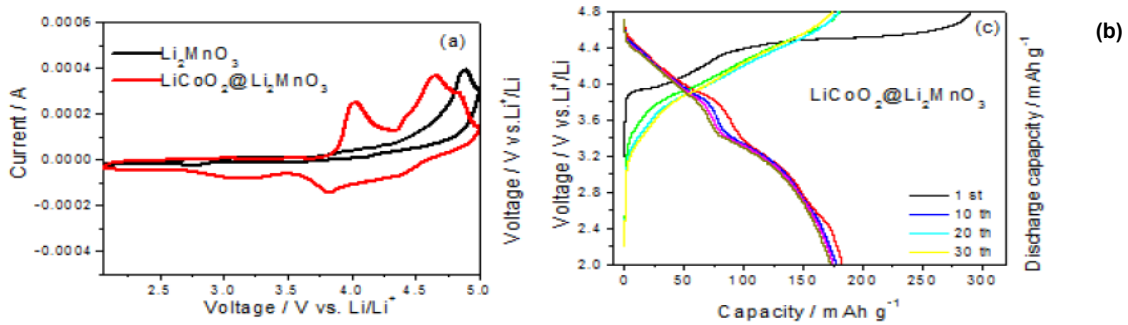

Figure 2.12: (a) CV voltammogram of Li_2MnO_3 and $LiCoO_2$@Li_2MnO_3, with the latter showing additional 3.8/4.0 V plateau attributed to the redox couple Co^{3+}/Co^{4+}. (b) Charge/discharge curve of $LiCoO_2$@Li_2MnO_3 [46]

2.1.3.4.3.3. Li/Mn/O site doping

Elemental doping has proved to be a good strategy to improve electrochemical performance of Li_2MnO_3 cathodes and table 2.4 summarizes some of the reports on the strategy. Doping can suppress oxygen loss and prevent structural transformation in Li_2MnO_3 which can lead to enhanced structural stability, electronic and ionic conductivity. In most cases, the least amount of dopant used gave the best results. When excess amounts of dopants are used, the crystal structure of the materials becomes distorted thus leading to instability and ultimately capacity loss. Therefore, doping with minimal amounts of dopants can suppress oxygen release and structural transformations which are responsible for the irreversible capacity loss during 1st cycling.

Transition metal doping

One of the first cases of transition metal doping was when Mori *et al.*[58] doped Li_2MnO_3 with varying amounts of Ruthenium (Ru) and observed a decrease in the electrical resistivity. The $Li_2Mn_{0.4}Ru_{0.6}O_3$ exhibited a discharge capacity of 192 $mAh.g^{-1}$ in the 1st cycle and 169 $mAh.g^{-1}$ in the 10th cycle at 1/10 C [58]. Since Mori *et al.* reported on $Li_2Mn_{0.4}Ru_{0.6}O_3$, several publications report on the doping of Li_2MnO_3 with transition metals (e.g., Fe, Co, Ti, Ni, Zr etc.) for enhanced performance [59],[62],[63],[64], [71].

In one first principle study, Gao *et al*. [65] showed that doping Li_2MnO_3 with molybdenum (Mo) greatly enhanced its properties as it resulted in a reduced band gap while at the same time inducing an increased number of electronic states in proximity of the Fermi level. As a result of this, Li-ion diffusion would increase, and the stability of oxygen would be enhanced leading to improved stability of the cathode material [65]. Ma *et al*. [66] also reported on the doping of Li_2MnO_3 with Molybdenum and obtained initial charge and discharge capacities of ~300 $mAh.g^{-1}$ and ~175 $mAh.g^{-1}$, respectively. The performance was attributed to the Mo ion expanding the lattice thus allowing increased Li^+ diffusion and lowering of de-lithiation potential which inhibits lattice oxygen loss.

Table 2.4: Comparison of different dopants materials and their enhancements.

Class of dopant	Dopant	Initial Discharge Capacity ($mAh.g^{-1}$)	Initial Coulombic Efficiency (%)	Retained Capacity ($mAh.g^{-1}$)	Rate Capacity ($mAh.g^{-1}$)	Measurement Conditions	Ref.
Transition Metal	Al	Up from 84 to 99.4	Up from 50 to 58.9	Up from 71.23 to 96.52	Up from 84.8 to 97.1	2.0 and 4.8 V, 20$mA.g^{-1}$, 40 cycles, RT	[57]
	Ru	Up from ~25 to 192	Down from ~71.43 to ~70.33	Improved	Improved	2.0 - 4.8 V, 20 mA. g^{-1}, 10 cycles, RT	[58]
	Ni	Up from ~28 to ~175	Up from ~56 to ~58.3	-	-	2.0 - 4.8 V, 10$mA.g^{-1}$, RT	[59]
	Mo	Up from ~37.5 to 175	Down from ~72.12 to 56	-	-	2.0 - 4.8 V, 10$mA.g^{-1}$, RT	[60]
Halogen	F	Up from 108 to 200	Down from 118.38 to 90.09	Up from ~94.7 to 184	Up from 66 to 125 (16C)	2.0 - 4.6 V, 10$mA.g^{-1}$,100 cycles, RT	[61]
Alkali/Alkali Earth Metals	Na	Up from 124.9 to 161	Up from 100 to 268.33	Up from 106.2 to 158.8	Up from 80.4 to 140.6 (1C)	2.0-4.6V, 10$mA.g^{-1}$, 100 cycles, RT	[30]
	Mg	Up from 241.9 to 307.5	Up from ~74.20 to ~87.85	Up from 187.96 to 259.84	Up from 102 to 123.1 (1C)	2.0-4.6V, 0.1C, 30 cycles, RT	[16]

Interestingly, aluminium (Al) doping at the manganese site was also found to greatly enhance electrochemical performance of Li_2MnO_3 [57]. In one study by Xiang *et al.* [57], it was revealed that due to the strong Al-O bond in the doped sample, the doping resulted in a weaker initial cycle capacity for the Al-doped sample. After the initial cycle, the cycling stability of the Al-doped sample is enhanced as depicted in figure 2.13 and the discharge capacity exceeded that of the pristine material. The EIS result of the Al-doped sample shows a reduction in the charge transfer resistance (R_{ct}) from 10037 to 5185 Ω indicating an increase in the charge transfer within the material. These results are in agreement with Kuganathan *et al.*'s findings which indicate that Al is a supreme dopant due to its small ionic radius, solution enthalpy and its trivalent oxidation state which can assist in creating an extra interstitial Li^+ ion in Li_2MnO_3 [19].

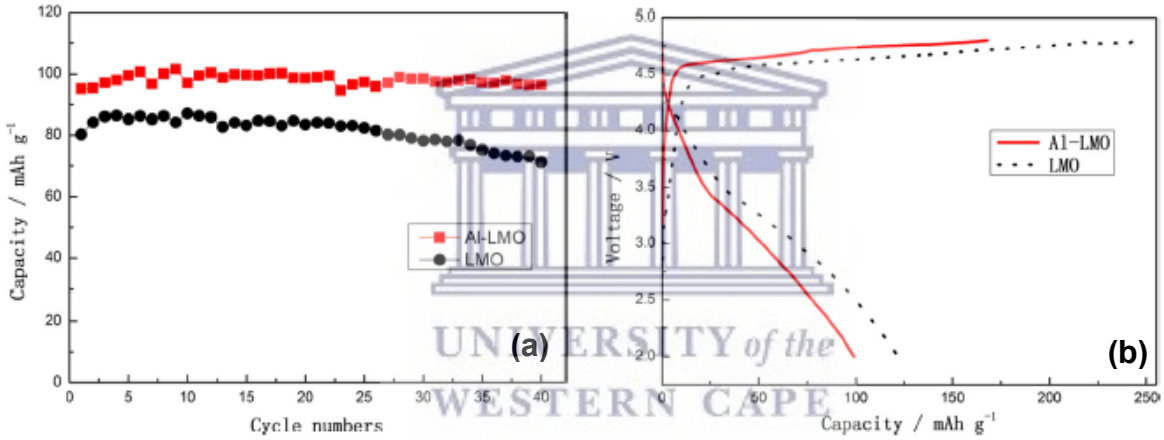

Figure 2.13: Cycling stability testing curves of Li_2MnO_3 and various Al-Li_2MnO_3 samples [57].

Matsunaga and co-workers also studied the effect of nickel- doping in Li_2MnO_3 compounds with varying Ni concentrations [59]. In their report, it was established that the charge and discharge capacities increased with the concentration of the Ni dopant (figure 2.14) [59]. This increase in performance was attributed to the ability of the nickel ion to lower the charge plateau potential therefore leading to higher first cycle charge capacities of up to ~300 $mAh.g^{-1}$ and discharge capacities of up to ~ 175 $mAh.g^{-1}$ [59].

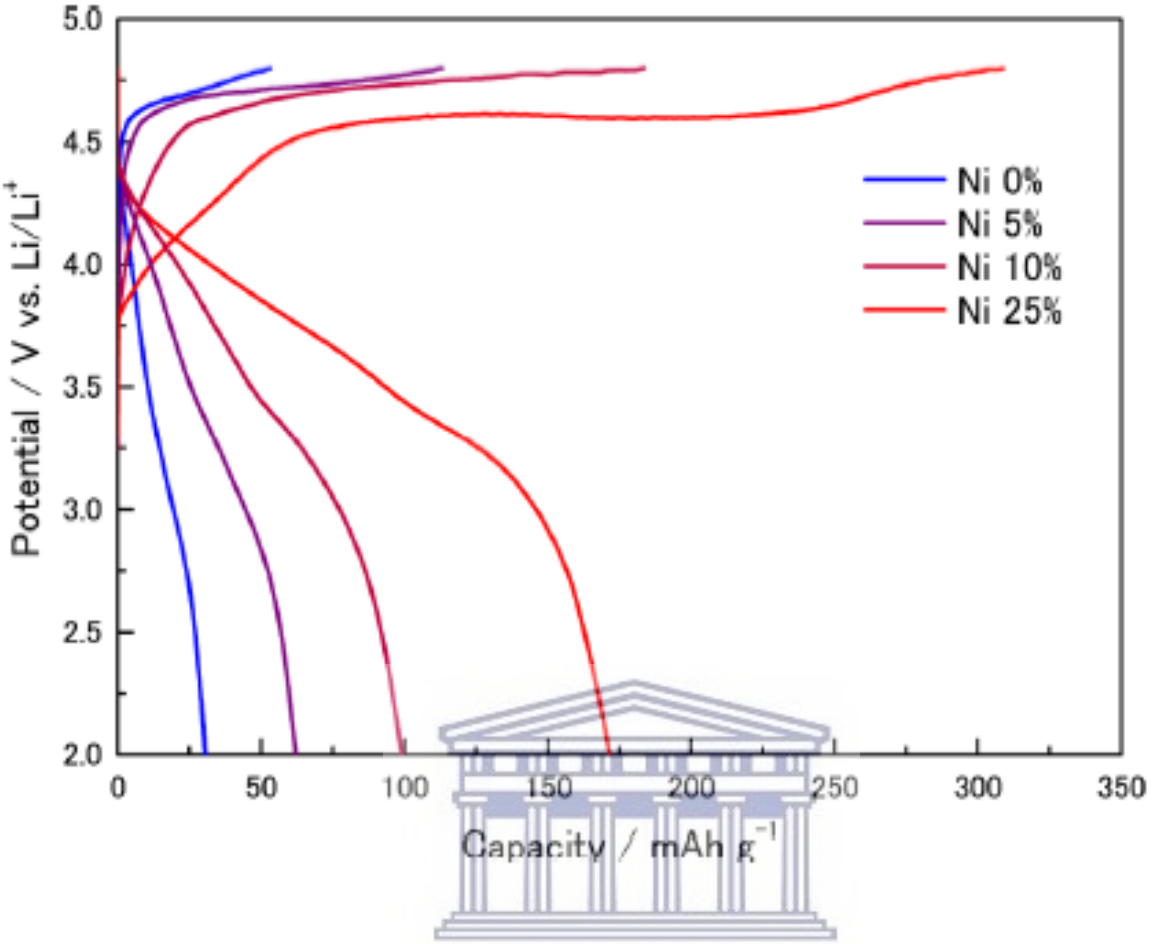

Figure 2.14: Initial Charge/discharge curves of Ni-Li_2MnO_3 [59].

Alkali/Alkaline-earth metal doping

Alkali/alkaline earth metal doping has been reported in several publications and focuses on the metal substitution at the lithium site as opposed to the manganese site [16], [67]. For example, figure 2.15 shows that substitution of some lithium ions with magnesium ions was performed to yield a material with the formula $Li_{1.98}Mg_{0.01}MnO_3$ which exhibited a higher initial discharge capacity of 307.5 mAh g^{-1} which exceeded the 241.9 mAh g^{-1} of the pristine Li_2MnO_3 material [16]. Improvement in the cycling stability was observed whereby an 84.5% capacity retention was recorded for the doped material [16]. The authors attributed the superior performance to the reduction in charge transfer resistance and the increase in the lithium ion diffusion coefficient [16].

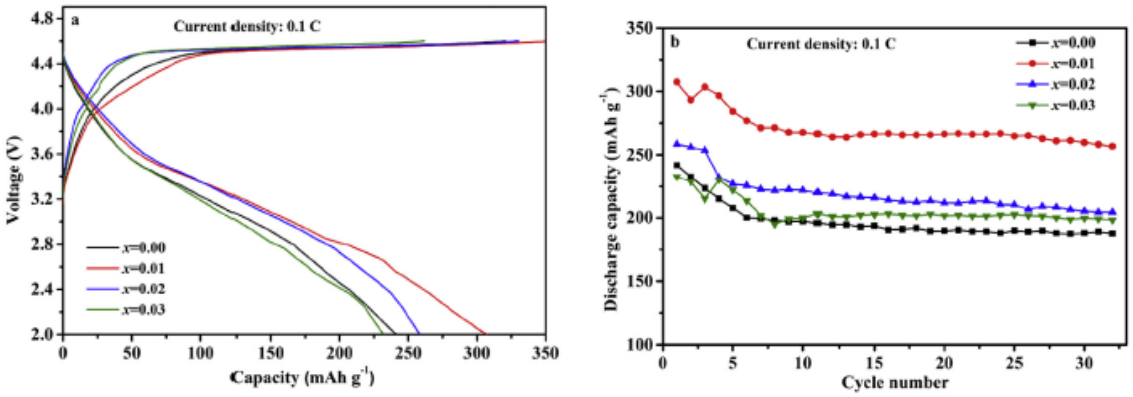

Figure 2.15: (a) Initial charge/discharge curves of Mg-Li_2MnO_3 and (b)Cycling stability testing of Mg-Li_2MnO_3 [16].

A similar type of substitution was performed by Dong *et al*. [30] when he synthesized the material $Li_{1.90}Na_{0.10}MnO_3$ by the partial substitution of lithium with sodium. The cathode material delivered a discharge capacity of 181 $mAh.g^{-1}$ in the 1st cycle and exhibited a high-capacity retention of 99.3% after cycling it 45 times at 1/10 C [30]. After 100 cycles at 1/2 C, a discharge capacity of 161 $mAh.g^{-1}$ was obtained indicating a 98.6% capacity retention [30]. The charge transfer resistance also decreased from 50.8 to 12.7 Ω.

Halogen Doping

Partial oxygen substitution with fluorine (F) has been investigated and found to be effective in enhancing the capacity of Li_2MnO_3 (figure 2.16) [61]. Dong *et al*. [16] reported that F doping weakened the Li-O bond and reduced the particle size of Li_2MnO_3 which shortens the pathway of Li^+ diffusion (figure 2.16). Moreover, F substitution increased Mn^{3+} species and oxygen vacancies leading to higher capacities and cycle stability as observed in Table 2.4. EIS Nyquist plots also reveal that the charge transfer resistance has decreased in the doped sample.

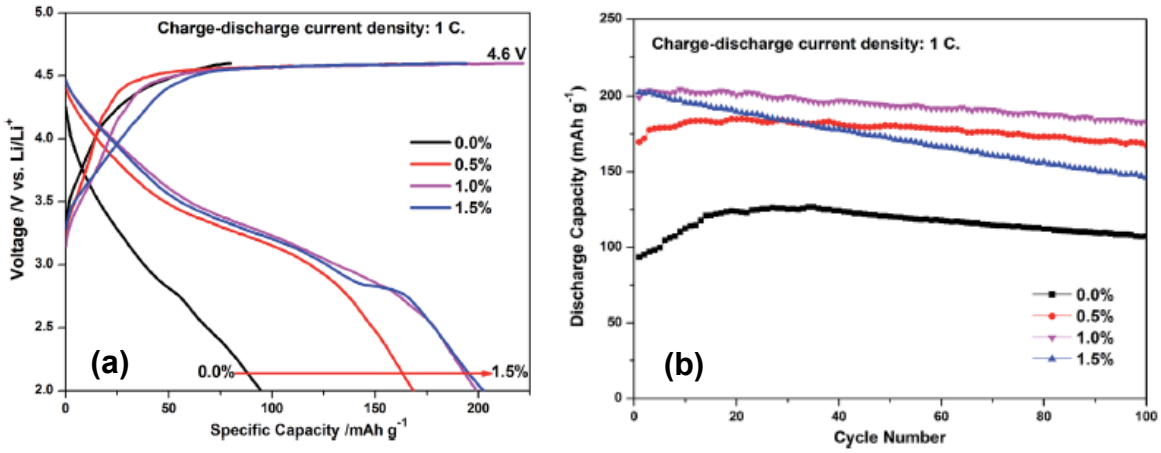

Figure 2.16: (a) Initial Charge/discharge curves of $Li_2MnO_{3-x}F_x$ and (b)Cycling stability testing of $Li_2MnO_{3-x}F_x$ [16].

Rare earth element doping

The use of rare earth elements such as Nd, Ce, Yb, Sc etc. to dope lithium ion cathode materials has been reported in several cathode materials, including $LiCoO_2$, $LiMn_2O_4$, $LiFePO_4$ and $xLi_2MnO_3(1-x)LiMO_2$ [68],[69],[70],[71]. As it stands, very few experimental reports have been published on rare earth element doping of pristine Li_2MnO_3 electrodes. From first principle studies, rare earth elements as dopants are favourable due to effects such as the ability to expand the lattice which helps to clear the pathway for diffusion thus facilitating ion transport [68],[69],[70],[71], [72], [73]. Furthermore, the expansion of the lattice slightly distorts the structure due to the large ionic radius which leads to smaller crystallites [72]. This offers the material a reduced charge transfer resistance and increased electric conductivity [68], [72].

A first principle study of the effects of rare earth doping was conducted by Zheng *et al.* [68], where they explored the effect of La, Ce, Pr and Sm on Li_2MnO_3. It was observed that La doping changed the properties of Li_2MnO_3 from semiconductor to metallic, while Ce, Pr and Sm doping retained the semiconductor nature [68]. In the case of the latter doped Li_2MnO_3, the band gap was significantly reduced compared to undoped samples which could be important in enhancing the electronic conductivity [68]. Similar results in improvement of electronic structure were observed by Yuzer *et al*. [74] when they experimentally doped Li_2MnO_3 with Nd, Ce and Yb. In their findings,

80 % Ce-doped Li_2MnO_3 showed a strong overlap of electronic levels that resulted in larger molecular bands [74].

It is worth noting that rare earth elements such as Pr, Sm, Nd, Ce, and Yb are favourable for doping as they possess redox couples i.e., RE^{3+}/RE^{2+} or RE^{4+}/RE^{3+} [72]. These redox couples can be electrochemically activated at appropriate potentials and can play a role as redox-active species thus increasing the energy density in cathode materials [72].

2.1.3.4.3.4. Other Modifications

Li_2MnO_3 dispersion

Li_2MnO_3 dispersion on rGO

Wei Zhao *et al*. [40] reported on the dispersion of pristine Li_2MnO_3 over reduced graphene oxide (rGO) to form a Li_2MnO_3/rGO composite as shown in Figure 2.17. Unlike merely coating the Li_2MnO_3 with rGO, their dispersion of Li_2MnO_3 particles over the rGO prevented agglomeration of Li_2MnO_3 particles thus improving the diffusion of lithium ions by shortening the path of diffusion [40]. The composite also showed improvement in the charge transfer resistance and exceptional discharge capacity in comparison with the pristine material [40]. The improved performance of the composite was attributed to the smaller particle size, reduced agglomeration, high surface area and electronic conductivity of rGO [40].

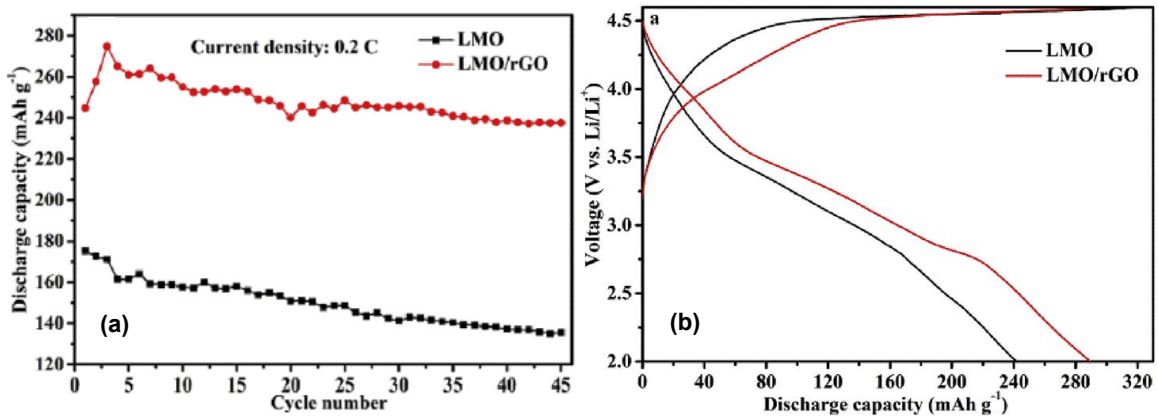

Figure 2.17: (a)Cycling stability testing of Li_2MnO_3 vs Li_2MnO_3/rGO (b) Initial charge/discharge curves of Li_2MnO_3 vs Li_2MnO_3/rGO [40].

Li_2MnO_3 dispersion on CNTs

In an effort to circumvent the agglomeration associated with nano structuring Li_2MnO_3 and improve its conductivity, Choi *et al*. [75] employed microwave assisted hydrothermal synthesis to form a composite of Li_2MnO_3 dispersed on Carbon Nanotubes (CNTs). The composite showed exceptional discharge capacities with electrochemical performance as observed in Table 2.5.

Table 2.5: Comparison of different dispersion substrates and their enhancements.

Substrate	Initial Discharge Capacity ($mAh.g^{-1}$)	Initial Coulombic Efficiency (%)	Retained Capacity ($mAh.g^{-1}$)	Capacity retention (%)	Measurement Conditions	Ref.
Reduced Graphene Oxide	289.4	96.7	250.62	86.6	2.0 and 4.6V, 0.1C, 45 cycles, RT	[39]
Carbon Nanotubes	273	70.54	196.19 (0.05C)	91.14 (0.05C)	2.8 - 5 V, 0.1C, 10 cycles, RT	[75]

2.1.3.4.4. Conclusion

This review has introduced Li_2MnO_3 based materials as possible high energy and high-capacity lithium ion battery cathode materials for electric vehicle and grid storage technologies. Furthermore, it highlighted the challenges associated with such materials including low initial coulombic efficiencies and irreversible capacity loss during cycling. From reviewing all the studies mentioned in this dissertation, it becomes increasingly clear that the performance of Li_2MnO_3 is strongly dependant on its surface properties. It can also be noted that various modifications such as surface coating, ionic doping, nano-structuring, and dispersion on conductive surfaces have the capability of greatly improving the low initial coulombic efficiencies, voltage fade and low-rate capacity associated with Li_2MnO_3 materials.

Furthermore, it has been demonstrated that in some instances the modified Li_2MnO_3 can attain an initial discharge capacity as high as 335 mAh g^{-1} which represents over 72 % of the theoretical capacity of Li_2MnO_3 (459 mAh g^{-1}) and 100% initial coulombic efficiencies. In other cases, Li_2MnO_3 was dispersed onto rGO and a capacity of >250 mAh $g^{-1}$was retained even after significant cycling representing >86% capacity retention. It is our belief that although each modification method has its merits and downfalls, Li_2MnO_3 materials would greatly benefit if these methods were exploited jointly. In conclusion, there is still a long way to go before the application of these materials become feasible in electric vehicle and grid storage technologies even with such exceptional results reported in this review. Firstly, we must better understand the origin of the electrochemical activity of such materials as this is still a highly debated matter. Secondly, the best optimum conditions must be established such as the synthesis methods and conditions, electrode thickness and coating/doping concentrations as they play a crucial role in determining the electrochemical performance.

References

1. Reddy, M.V., Mauger, A., Julien, C.M., Paolella, A. and Zaghib, K., 2020. Brief history of early lithium-battery development. *Materials*, 13(8), p.1884.
2. Deng, D., 2015. Li-ion batteries: basics, progress, and challenges. *Energy Science & Engineering*, 3(5), pp.385-418.
3. Abraham, K.M., 1993. Directions in secondary lithium battery research and development. *Electrochimica Acta*, 38(9), pp.1233-1248.
4. Scrosati, B., 2011. History of lithium batteries. *Journal of solid-state electrochemistry*, 15(7), pp.1623-1630.
5. Balasubramaniam, B., Singh, N., Verma, S. and Gupta, R.K., 2020. Recycling of lithium from Li-ion batteries.
6. ECS. 2021. *Exploding Hoverboards Explained - ECS*. [online] Available at: <https://www.electrochem.org/exploding-hoverboards-explained> [Accessed 9 March 2021].
7. Notohara, H., Urita, K. and Moriguchi, I., 2020. Tin oxide electrodes in Li and Na-ion batteries. *In Tin Oxide Materials*, pp. 411-439, Elsevier.

8. Marcinek, M., Syzdek, J., Marczewski, M., Piszcz, M., Niedzicki, L., Kalita, M., Plewa-Marczewska, A., Bitner, A., Wieczorek, P., Trzeciak, T. and Kasprzyk, M., 2015. Electrolytes for Li-ion transport–Review. *Solid State Ionics*, 276, pp.107-126.
9. Li, Q., Chen, J., Fan, L., Kong, X. and Lu, Y., 2016. Progress in electrolytes for rechargeable Li-based batteries and beyond. *Green Energy & Environment*, 1(1), pp.18-42.
10. Mit Engineering. 2021. MIT School of Engineering | » How does a battery work? [online] Available at: <https://engineering.mit.edu/engage/ask-an-engineer/how-does-a-batterywork/#: ~:text=The%20electrolyte%20is%20a%20chemical, electrical%20energy%20to%20the%20device.> [Accessed 10 March 2021].
11. Warner, J.T., 2019. Lithium-Ion Battery Chemistries: A Primer. Elsevier. pp. 139-170.
12. Lü, X., Xia, B., Liu, C., Yang, Y. and Tang, H., 2016. TiO_2-based nanomaterials for advanced environmental and energy-related applications.
13. Wu, F., Li, N., Su, Y., Zhang, L., Bao, L., Wang, J., Chen, L., Zheng, Y., Dai, L., Peng, J. and Chen, S., 2014. Ultrathin spinel membrane-encapsulated layered lithium-rich cathode material for advanced Li-ion batteries. *Nano letters,* 14(6), pp.3550-3555.
14. Ram, P., Gören, A., Ferdov, S., Silva, M.M., Singhal, R., Costa, C.M., Sharma, R.K. and Lanceros-Méndez, S., 2016. Improved performance of rare earth doped $LiMn_2O_4$ cathodes for lithium-ion battery applications. *New Journal of Chemistry*, 40(7), pp.6244-6252.
15. Zhu, L., Ran, R., Tade, M., Wang, W. and Shao, Z., 2016. Perovskite materials in energy storage and conversion. *Asia-Pacific Journal of Chemical Engineering*, 11(3), pp.338-369.
16. Zhao, W., Xiong, L., Xu, Y., Xiao, X., Wang, J. and Ren, Z., 2016. Magnesium substitution to improve the electrochemical performance of layered Li_2MnO_3 positive-electrode material. *Journal of Power Sources*, 330, pp.37-44.
17. Lan, X., Xin, Y., Wang, L. and Hu, X., 2018. Nanoscale surface modification of Li-rich layered oxides for high-capacity cathodes in Li-ion batteries. *Journal of Nanoparticle Research,* 20(3), pp.1-38.

18. Kuganathan, N., Sgourou, E.N., Panayiotatos, Y. and Chroneos, A., 2019. Defect Process, Dopant Behaviour and Li Ion Mobility in the Li_2MnO_3 Cathode Material. *Energies*, 12(7), p.1329.
19. Chen, Z., Zhang, W. and Yang, Z., 2019. A review on cathode materials for advanced lithium ion batteries: microstructure designs and performance regulations. *Nanotechnology*, 31(1), p.012001.
20. Pan, H., Zhang, S., Chen, J., Gao, M., Liu, Y., Zhu, T. and Jiang, Y., 2018. Li-and Mn-rich layered oxide cathode materials for lithium-ion batteries: a review from fundamentals to research progress and applications. *Molecular Systems Design & Engineering*, 3(5), pp.748-803.
21. Song, Y., Zhao, X., Wang, C., Bi, H., Zhang, J., Li, S., Wang, M. and Che, R., 2017. Insight into the atomic structure of Li_2MnO_3 in Li-rich Mn-based cathode materials and the impact of its atomic arrangement on electrochemical performance. *Journal of Materials Chemistry A*, 5(22), pp.11214-11223.
22. Koyama, Y., Tanaka, I., Nagao, M. and Kanno, R., 2009. First-principles study on lithium removal from Li_2MnO_3. Journal of Power Sources, 189(1), pp.798-801.
23. Julien, C., Mauger, A., Vijh, A. and Zaghib, K., 2016. *Lithium batteries*. In Lithium batteries (pp. 29-68). Springer, Cham.
24. Robertson, A.D. and Bruce, P.G., 2002. The origin of electrochemical activity in Li_2MnO_3. *Chemical communications*, (23), pp.2790-2791.
25. Ozoemena, K.I. and Chen, S. eds., 2016. Nanomaterials in advanced batteries and supercapacitors, pp. p-567, Switzerland: Springer International Publishing.
26. Zuo, Y., Li, B., Jiang, N., Chu, W., Zhang, H., Zou, R. and Xia, D., 2018. A high-capacity O_2-type Li-rich cathode material with a single-layer Li_2MnO_3 superstructure. *Advanced materials*, 30(16), p.1707255.
27. Liu, G. and Zhang, S., 2016. One-step Synthesis of Low-cost and High Active Li_2MnO_3 Cathode Materials. *International Journal of Electrochemistry Science*, 11, pp.5545-5551.
28. Serrano-Sevillano, J., Reynaud, M., Saracibar, A., Altantzis, T., Bals, S., van Tendeloo, G. and Casas-Cabanas, M., 2018. Enhanced electrochemical performance of Li-rich cathode materials through microstructural control. *Physical Chemistry Chemical Physics*, 20(35), pp.23112-23122.
29. Sun, Y., Cong, H., Zan, L. and Zhang, Y., 2017. Oxygen vacancies and stacking faults introduced by low-temperature reduction improve the electrochemical

properties of Li_2MnO_3 nanobelts as lithium-ion battery cathodes. *ACS applied materials & interfaces*, 9(44), pp.38545-38555.

30. Dong, X., Xu, Y., Xiong, L., Sun, X. and Zhang, Z., 2013. Sodium substitution for partial lithium to significantly enhance the cycling stability of Li_2MnO_3 cathode material. *Journal of Power Sources*, 243, pp.78-87.
31. Rana, J., Stan, M., Kloepsch, R., Li, J., Schumacher, G., Welter, E., Zizak, I., Banhart, J. and Winter, M., 2014. Structural changes in Li_2MnO_3 cathode material for Li-Ion batteries. *Advanced Energy Materials*, 4(5), p.1300998.
32. Yu, D.Y.W., Yanagida, K., Kato, Y. and Nakamura, H., 2009. Electrochemical activities in Li_2MnO_3. Journal of The Electrochemical Society, 156(6), p.A417.
33. Chen, H. and Islam, M.S., 2016. Lithium extraction mechanism in Li-rich Li_2MnO_3 involving oxygen hole formation and dimerization. *Chemistry of Materials*, 28(18), pp.6656-6663.
34. Fichtner, M., 2011. Nanoconfinement effects in energy storage materials. *Physical Chemistry Chemical Physics*, 13(48), pp.21186-21195.
35. Bazito, F.F. and Torresi, R.M., 2006. Cathodes for lithium ion batteries: the benefits of using nanostructured materials. *Journal of the Brazilian Chemical Society*, 17(4), pp.627-642.
36. Mahmood, N. and Hou, Y., 2014. Electrode nanostructures in lithium-based batteries. *Advanced Science*, 1(1), p.1400012.
37. Sayle, T.X., Caddeo, F., Monama, N.O., Kgatwane, K.M., Ngoepe, P.E. and Sayle, D.C., 2015. Origin of electrochemical activity in nano-Li_2MnO_3; stabilization via a 'point defect scaffold'. *Nanoscale*, 7(3), pp.1167-1180.
38. Zhang, F., 2017. Grand challenges for nanoscience and nanotechnology in energy and health. *Frontiers in chemistry*, 5, p.80.
39. Freire, M., Lebedev, O.I., Maignan, A., Jordy, C. and Pralong, V., 2017. Nanostructured Li_2MnO_3: a disordered rock salt type structure for high energy density Li ion batteries. *Journal of Materials Chemistry A*, 5(41), pp.21898-21902.
40. Zhao, W., Xiong, L., Xu, Y., Li, H. and Ren, Z., 2017. High performance Li_2MnO_3/rGO composite cathode for lithium ion batteries. *Journal of Power Sources*, 349, pp.11-17.
41. Lim, J., Moon, J., Gim, J., Kim, S., Kim, K., Song, J., Kang, J., Im, W.B. and Kim, J., 2012. Fully activated Li_2MnO_3 nanoparticles by oxidation reaction. *Journal of Materials Chemistry*, 22(23), pp.11772-11777.

42. Yao, L., Yu, Z., Qian, J. and Liu, H., 2013. Synthesis of Nano-Sized Li_2MnO_3 Powders by Citrate-Ntrate Gel Combustion Process and Their Electrochemical Properties. *In Solid State Ionics: Ionics for Sustainable World*,p. 96-101.
43. Wu, X., Li, H., Fei, H., Zheng, C. and Wei, M., 2014. Facile synthesis of Li_2MnO_3 nanowires for lithium-ion battery cathodes. *New Journal of Chemistry*, 38(2), pp.584-587.
44. Vendra, V.K., Nguyen, T.Q., Thapa, A.K., Jasinski, J.B. and Sunkara, M.K., 2015. Scalable synthesis and surface stabilization of Li_2MnO_3 NWs as high rate cathode materials for Li-ion batteries. *RSC Advances*, 5(46), pp.36906-36912.
45. Wang, F., Xiao, S., Li, M., Wang, X., Zhu, Y., Wu, Y., Shirakawa, A. and Peng, J., 2015. A nanocomposite of Li_2MnO_3 coated by $FePO_4$ as cathode material for lithium ion batteries. *Journal of Power Sources*, 287, pp.416-421.
46. Wang, F.X., Xiao, S.Y., Chang, Z., Li, M.X., Wu, Y.P. and Holze, R., 2014. Coaxial $LiCoO_2$@ Li_2MnO_3 nanoribbon as a high capacity cathode for lithium ion batteries. *International Journal of Electrochemical Science*, 9, pp.6182-6190.
47. Menon, A.S., Ojwang, D.O., Willhammar, T., Peterson, V.K., Edstrom, K., Gomez, C.P. and Brant, W.R., 2020. Influence of Synthesis Routes on the Crystallography, Morphology, and Electrochemistry of Li_2MnO_3. *ACS applied materials & interfaces*, 12(5), pp.5939-5950.
48. Matsunaga, T., Komatsu, H., Shimoda, K., Minato, T., Yonemura, M., Kamiyama, T., Kobayashi, S., Kato, T., Hirayama, T., Ikuhara, Y. and Arai, H., 2016. Dependence of structural defects in Li_2MnO_3 on synthesis temperature. *Chemistry of Materials*, 28(12), pp.4143-4150.
49. SShi, S.J., Tu, J.P., Tang, Y.Y., Liu, X.Y., Zhang, Y.Q., Wang, X.L. and Gu, C.D., 2013. Enhanced cycling stability of $Li[Li_{0.2}Mn_{0.54}Ni_{0.13}Co_{0.13}]O_2$ by surface modification of MgO with melting impregnation method. *Electrochimica Acta*, 88, pp.671-679.
50. Zhang, Y., Li, Y., Xia, X., Wang, X., Gu, C. and Tu, J., 2015. High-energy cathode materials for Li-ion batteries: a review of recent developments. *Science China Technological Sciences*, 58(11), pp.1809-1828.
51. Xiong, L., Sun, M., Xu, Y., Du, X. and Xiao, X., 2018. Synthesis of carbon coated Li_2MnO_3 cathode material with enhanced rate capability for lithium-ion batteries. *Solid State Ionics*, 325, pp.170-175.

52. Wang, F., Chang, Z., Wang, X., Wang, Y., Chen, B., Zhu, Y. and Wu, Y., 2015. Composites of porous Co_3O_4 grown on Li_2MnO_3 microspheres as cathode materials for lithium ion batteries. *Journal of Materials Chemistry A*, 3(9), pp.4840-4845.
53. Lee, J.E., Kim, M.C., Moon, S.H., Kim, E.S., Shin, Y.K., Choi, S., Kwon, S.H., Kim, S.J., Kwon, H.J., and Park, K.W., 2019. Role of polyvinylpyrrolidone in the electrochemical performance of Li_2MnO_3 cathode for lithium-ion batteries. *RSC advances*, 9(18), pp.10297-10304.
54. Kim, S.J., Kim, M.C., Kwak, D.H., Kim, D.M., Lee, G.H., Choe, H.S. and Park, K.W., 2016. Highly stable TiO_2 coated Li_2MnO_3 cathode materials for lithium-ion batteries. *Journal of Power Sources*, 304, pp.119-127.
55. Xiong, L., Sun, M., Xu, Y., Du, X. and Xiao, X., 2018. Synthesis of carbon coated Li_2MnO_3 cathode material with enhanced rate capability for lithium-ion batteries. *Solid State Ionics*, 325, pp.170-175.
56. Ning, F., Shang, H., Li, B., Jiang, N., Zou, R. and Xia, D., 2019. Surface thermodynamic stability of Li-rich Li_2MnO_3: effect of defective graphene. *Energy Storage Materials*, 22, pp.113-119.
57. Xiang, Y. and Wu, X., 2018. Enhanced electrochemical performances of Li_2MnO_3 cathode materials by Al doping. *Ionics*, 24(1), pp.83-89.
58. Mori, D., Sakaebe, H., Shikano, M., Kojitani, H., Tatsumi, K. and Inaguma, Y., 2011. Synthesis, phase relation and electrical and electrochemical properties of ruthenium substituted Li_2MnO_3 as a novel cathode material. *Journal of Power Sources*, 196(16), pp.6934-6938.
59. Matsunaga, T., Komatsu, H., Shimoda, K., Minato, T., Yonemura, M., Kamiyama, T., Kobayashi, S., Kato, T., Hirayama, T., Ikuhara, Y. and Arai, H., 2016. Structural understanding of superior battery properties of partially Ni-doped Li_2MnO_3 as cathode material. *The Journal Of Physical Chemistry Letters*, 7(11), pp.2063-2067.
60. Ma, J., Zhou, Y.N., Gao, Y., Kong, Q., Wang, Z., Yang, X.Q. and Chen, L., 2014. Molybdenum substitution for improving the charge compensation and activity of Li_2MnO_3. *Chemistry–A European Journal*, 20(28), pp.8723-8730.
61. Dong, X., Xu, Y., Yan, S., Mao, S., Xiong, L. and Sun, X., 2015. Towards low-cost, high energy density Li_2MnO_3 cathode materials. *Journal of Materials Chemistry A*, 3(2), pp.670-679.

62. Dong, X., Xu, Y., Yan, S., Mao, S., Xiong, L. and Sun, X., 2015. Towards low-cost, high energy density Li_2MnO_3 cathode materials. *Journal of Materials Chemistry A*, 3(2), pp.670-679.

Dahiya, P.P., Ghanty, C., Sahoo, K., Basu, S. and Majumder, S.B., 2018. Suppression of voltage decay and improvement in electrochemical performance by zirconium doping in Li-rich cathode materials for Li-ion batteries. *Journal of The Electrochemical Society*, 165(13), p.A3114.

63. Tabuchi, M., Kageyama, H., Takamori, K., Imanari, Y. and Nakane, K., 2016. Synthesis and electrochemical characterization of Ni-and Ti-substituted Li_2MnO_3 positive electrode material using coprecipitation–hydrothermal–calcination method. *Electrochimica Acta*, 210, pp.105-110.

64. Yu, Z., Shang, S.L., Gordin, M.L., Mousharraf, A., Liu, Z.K. and Wang, D., 2015. Ti-substituted Li $[Li_{0.26}Mn_{0.6-x}Ti_xNi_{0.07}Co_{0.07}]O_2$ layered cathode material with improved structural stability and suppressed voltage fading. *Journal of Materials Chemistry A*, 3(33), pp.17376-17384.

65. Gao, Y., Ma, J., Wang, X., Lu, X., Bai, Y., Wang, Z. and Chen, L., 2014. Improved electron/Li-ion transport and oxygen stability of Mo-doped Li_2MnO_3. *Journal of Materials Chemistry A*, 2(13), pp.4811-4818.

66. Hou, J., Park, M.H., Zhang, S., Yao, Y., Chen, L.M., Li, J.H. and Yang, Y., 2008. Bandgap and molecular energy level control of conjugated polymer photovoltaic materials based on benzo [1,2-b:4,5-b′]dithiophene. *Macromolecules*, 41(16), pp.6012-6018.

67. Wu, S.Q., Zhu, Z.Z., Yong, Y.A.N.G. and Hou, Z.F., 2009. Effects of Na-substitution on structural and electronic properties of Li_2CoSiO_4 cathode material. *Transactions of Nonferrous Metals Society of China*, 19(1), pp.182-186.

68. Lu-Min, Z., Shu-Ping, Z., Bo, X. and Chu-Ying, O., 2019. First-principles study of rare-earth-doped cathode materials Li_2MnO_3 in Li-ion batteries. *Acta Physica Sinica*, 68(13), pp. 1–9, 2019.

69. Huiyong, L.I.U., Ganqun, D.E.N.G. and Yonglang, G.U.O., 2008. Influence of Sc^{3+} on $LiMn_2O_4$ cathode materials at elevated temperature. *Journal of Rare Earths*, 26(5), pp.722-726.

70. Çelik, G., Aktaş, S., Ateş, Ş., Özkendir, O.M. and Klysubun, W., 2019. Crystal and electronic structure study of the $Li_2Mn_{1-x}Nd_xO_3$ battery cathode. *Progress in Natural Science: Materials International*, 29(2), pp.119-123.

71. Ding, Y., Zhang, P., Jiang, Y. and Gao, D., 2007. Effect of rare earth elements doping on structure and electrochemical properties of $LiNi_{1/3}Co_{1/3}Mn_{1/3}O_2$ for lithium-ion battery. *Solid State Ionics*, 178(13-14), pp.967-971.
72. Zhao, H., Xia, J., Yin, D., Luo, M., Yan, C. and Du, Y., 2019. Rare earth incorporated electrode materials for advanced energy storage. *Coordination Chemistry Reviews*, 390, pp.32-49.
73. Shuting, Y., 2003. Effect of Rare Earth Elements Doping on Structure and Electrochemical Properties of $LiMn_2O_4$ Materials for the Li-ion Battery. *Journal-Chinese Rare Earth Society-Chinese Edition-*, 21(4), pp.413-416.
74. Yuzer, A. and Ozkendir, O.M., 2016. Influence of Rare-Earth Substitution on the Crystal and Electronic Properties of a Li_2MnO_3 Battery Cathode. *Journal of Electronic Materials*, 45(2), pp.989-998.
75. Choi, A., Palanisamy, K., Kim, Y., Yoon, J., Park, J.H., Lee, S.W., Yoon, W.S. and Kim, K.B., 2014. Microwave-assisted hydrothermal synthesis of electrochemically active nano-sized Li_2MnO_3 dispersed on carbon nanotube network for lithium ion batteries. *Journal of alloys and compounds*, 591, pp.356-361.